

# Probing Neutral Triple Gauge Couplings with $Z^*\gamma(\nu\bar{\nu}\gamma)$ Production at Hadron Colliders

John Ellis <sup>a</sup>, Hong-Jian He <sup>b</sup>, Rui-Qing Xiao <sup>c</sup>

<sup>a</sup> Department of Physics, King's College London, Strand, London WC2R 2LS, UK;  
Theoretical Physics Department, CERN, CH-1211 Geneva 23, Switzerland;  
T. D. Lee Institute, Shanghai Jiao Tong University, Shanghai, China

<sup>b</sup> T. D. Lee Institute and School of Physics & Astronomy,  
Key Laboratory for Particle Astrophysics and Cosmology,  
Shanghai Key Laboratory for Particle Physics and Cosmology,  
Shanghai Jiao Tong University, Shanghai, China;  
Physics Department & Institute of Modern Physics, Tsinghua University, Beijing, China;  
Center for High Energy Physics, Peking University, Beijing, China

<sup>c</sup> Department of Physics, King's College London, Strand, London WC2R 2LS, UK;  
T. D. Lee Institute and School of Physics & Astronomy,  
Shanghai Jiao Tong University, Shanghai, China

(john.ellis@cern.ch, hjhe@sjtu.edu.cn, xiaoruiqing@sjtu.edu.cn)

## Abstract

We study probes of neutral triple gauge couplings (nTGCs) via  $Z^*\gamma$  production followed by off-shell decays  $Z^* \rightarrow \nu\bar{\nu}$  at the LHC and future  $pp$  colliders, including both CP-conserving (CPC) and CP-violating (CPV) couplings. We present the dimension-8 SMEFT operators contributing to nTGCs and derive the correct form factor formulation for the off-shell vertices  $Z^*\gamma V^*$  ( $V = Z, \gamma$ ) by matching them with the dimension-8 SMEFT operators. Our analysis includes new contributions enhanced by the large off-shell momentum of  $Z^*$ , beyond those of the conventional  $Z\gamma V^*$  vertices with on-shell  $Z\gamma$ . We analyze the sensitivity reaches for probing the CPC/CPV nTGC form factors and the new physics scales of the dimension-8 nTGC operators at the LHC and future 100 TeV  $pp$  colliders. We compare our predictions with the existing LHC measurements of CPC nTGCs in the  $\nu\bar{\nu}\gamma$  channel and demonstrate the importance of our new method.

# 1 Introduction

Neutral triple gauge couplings (nTGCs) are attracting increased theoretical and experimental interest [1][2][3][4][5][6]. This is largely driven by the fact [7][8] that the nTGCs do not appear in the Standard Model (SM) Lagrangian, nor do they show up in the dimension-6 Lagrangian of the SM Effective Field Theory (SMEFT) [9], suggesting that they could open a unique new window on physics beyond the SM that may first appear at the dimension-8 level. The SMEFT provides a powerful universal framework to formulate model-independently such new physics beyond the SM, by parametrizing the low-energy effects of possible high-mass new physics in terms of operators composed of the SM fields that incorporate the full  $SU(3)\otimes SU(2)\otimes U(1)$  gauge symmetry of the SM.

There have been extensive studies of the dimension-6 operators [9][10][11] in the SMEFT, including the experimental constraints on their coefficients and hence on the associated new physics cutoff scale  $\Lambda$ . But these studies do not involve nTGCs because they first appear as a set of dimension-8 operators of the SMEFT. In general, dimension-8 operators make interference contributions to amplitudes at  $O(1/\Lambda^4)$ , and thus can contribute to cross sections at the same order. But dimension-6 SMEFT operators contributing to amplitudes at  $O(1/\Lambda^2)$  also contribute to cross sections at  $O(1/\Lambda^4)$  in general, complicating efforts to isolate any dimension-8 contributions. The absence of dimension-6 contributions to nTGCs avoids this complication, making them an ideal place to probe the new physics at dimension-8 level.

Previous phenomenological studies of nTGCs in the SMEFT formalism have mainly focused on CP-conserving (CPC) operators that contribute to scattering amplitudes involving the neutral triple gauge vertex (nTGV)  $Z\gamma V^*$  ( $V=Z, \gamma$ ) through the reaction  $f\bar{f}\rightarrow Z\gamma$ . In the case of  $e^+e^-$  colliders, on-shell  $Z\gamma$  production with  $Z\rightarrow \ell^-\ell^+, \nu\bar{\nu}, q\bar{q}$  final states have been considered, but at  $pp$  colliders off-shell invisible decays  $Z^*\rightarrow \nu\bar{\nu}$  cannot be separated from on-shell  $Z$  decays because of the insufficient kinematic information of  $Z$  boson. Hence, for the  $\nu\bar{\nu}\gamma$  channel it is important to include the off-shell production of  $Z^*\rightarrow \nu\bar{\nu}$  at  $pp$  colliders.

In this work, we study the nTGVs with two off-shell bosons,  $Z^*\gamma V^*$  ( $V=Z, \gamma$ ), which include contributions from additional dimension-8 operators that were not considered in the previous nTGC studies. We include a new analysis of CP-violating (CPV) nTGCs. As the basis for this work, we first formulate the correct CPC and CPV form factors of the nTGC vertices  $Z^*\gamma V^*$  that are compatible with the full electroweak  $SU(2)\otimes U(1)$  gauge symmetry of the SM [12]. By matching the CPC and CPV dimension-8 nTGC operators with the corresponding nTGC form factors, we derive the correct formulations of the CPC and CPV  $Z^*\gamma V^*$  form factors. We then use these formulations to study the sensitivity reaches of the LHC and the projected 100 TeV  $pp$  colliders for probing the CPC and CPV nTGCs through the reaction  $pp(q\bar{q})\rightarrow Z^*\gamma\rightarrow \nu\bar{\nu}\gamma$ . We further compare our predictions with the existing LHC measurements [5] of CPC nTGCs in the  $\nu\bar{\nu}\gamma$  channel, and clarify the importance of using our new nTGC form factor formulation for the correct LHC experimental analysis.

## 2 Formulating $Z^*\gamma V^*$ Form Factors from Matching the SMEFT

In previous works [1][2][3], we studied the dimension-8 SMEFT operators that generate nTGCs and their contributions to  $Z\gamma$  production at the LHC and future colliders. In particular, we studied systematically  $Z\gamma V^*$  vertices including their matching with the corresponding SMEFT operators and the correct formulation of nTGC form factors that respect the full electroweak

SU(2)⊗U(1) gauge symmetry of the SM. However, unlike the case of  $e^+e^-$  collisions where the on-shell constraint can be imposed on the invisible decays of  $Z \rightarrow \nu\bar{\nu}$ , this is not possible in  $pp$  collisions, for which only the missing transverse momentum can be measured. Moreover, since  $Z$  boson is an unstable particle, the invariant-masses of  $\ell^+\ell^-$  and  $q\bar{q}$  final states from  $Z$  decays are not exactly on-shell, in general. For these reasons, it is important to study the nTGVs with the final-state  $Z^*$  off-shell, as well as the initial-state  $V^*$ .

The general dimension-8 SMEFT Lagrangian takes the following form:

$$\Delta\mathcal{L}(\text{dim-8}) = \sum_j \frac{\tilde{c}_j}{\tilde{\Lambda}^4} \mathcal{O}_j = \sum_j \frac{\text{sign}(\tilde{c}_j)}{\Lambda_j^4} \mathcal{O}_j = \sum_j \frac{1}{[\Lambda_j^4]} \mathcal{O}_j, \quad (2.1)$$

where the dimensionless coefficients  $\tilde{c}_j$  may take either sign,  $\text{sign}(\tilde{c}_j) = \pm$ . For each dimension-8 operator  $\mathcal{O}_j$ , we define in Eq.(2.1) the corresponding effective cutoff scale for new physics,  $\Lambda_j \equiv \tilde{\Lambda}/|\tilde{c}_j|^{1/4}$ , and introduce the notation  $[\Lambda_j^4] \equiv \text{sign}(\tilde{c}_j)\Lambda_j^4$ .

The following CPC and CPV nTGC operators include Higgs doublets:

$$\text{CPC: } \mathcal{O}_{\tilde{B}W} = iH^\dagger \tilde{B}_{\mu\nu} W^{\mu\rho} \{D_\rho, D^\nu\} H + \text{h.c.}, \quad (2.2a)$$

$$\text{CPC: } \mathcal{O}_{\tilde{B}\tilde{W}} = iH^\dagger (D_\sigma \tilde{W}_{\mu\nu}^a W^{a\mu\sigma} + D_\sigma \tilde{B}_{\mu\nu} B^{\mu\sigma}) D^\nu H + \text{h.c.}, \quad (2.2b)$$

$$\text{CPV: } \tilde{\mathcal{O}}_{BW} = iH^\dagger B_{\mu\nu} W^{\mu\rho} \{D_\rho, D^\nu\} H + \text{h.c.}, \quad (2.2c)$$

$$\text{CPV: } \tilde{\mathcal{O}}_{WW} = iH^\dagger W_{\mu\nu} W^{\mu\rho} \{D_\rho, D^\nu\} H + \text{h.c.}, \quad (2.2d)$$

$$\text{CPV: } \tilde{\mathcal{O}}_{BB} = iH^\dagger B_{\mu\nu} B^{\mu\rho} \{D_\rho, D^\nu\} H + \text{h.c.}, \quad (2.2e)$$

where  $H$  denotes the Higgs doublet of the SM. The operators (2.2a) and (2.2c)-(2.2e) were given in [8], to which we have further added an independent CPC operator (2.2b).

The following are the dimension-8 CPC and CPV nTGC operators that contain pure gauge fields only:

$$\text{CPC: } g\mathcal{O}_{G+} = \tilde{B}_{\mu\nu} W^{a\mu\rho} (D_\rho D_\lambda W^{a\nu\lambda} + D^\nu D^\lambda W_{\lambda\rho}^a), \quad (2.3a)$$

$$\text{CPC: } g\mathcal{O}_{G-} = \tilde{B}_{\mu\nu} W^{a\mu\rho} (D_\rho D_\lambda W^{a\nu\lambda} - D^\nu D^\lambda W_{\lambda\rho}^a), \quad (2.3b)$$

$$\text{CPV: } g\tilde{\mathcal{O}}_{G+} = B_{\mu\nu} W^{a\mu\rho} (D_\rho D_\lambda W^{a\nu\lambda} + D^\nu D^\lambda W_{\lambda\rho}^a), \quad (2.3c)$$

$$\text{CPV: } g\tilde{\mathcal{O}}_{G-} = B_{\mu\nu} W^{a\mu\rho} (D_\rho D_\lambda W^{a\nu\lambda} - D^\nu D^\lambda W_{\lambda\rho}^a), \quad (2.3d)$$

where the operators ( $\mathcal{O}_{G+}, \mathcal{O}_{G-}$ ) are CPC [2], and the new operators ( $\tilde{\mathcal{O}}_{G+}, \tilde{\mathcal{O}}_{G-}$ ) are CPV.

The conventional formalism for nTGC form factors was proposed over 20 years ago [7] and respects only the residual gauge symmetry  $U(1)_{\text{em}}$ . However, as we stressed in Ref. [1], it does not respect the full electroweak SU(2)⊗U(1) gauge symmetry of the SM, and leads to unphysical large high-energy behaviors of certain scattering amplitudes [1]. We thus proposed [1] a new formulation of the CPC form factors of the nTGVs  $Z\gamma V^*$  that is compatible with the full SM gauge group with spontaneous electroweak symmetry breaking. We will construct an extended formulation to include the CPV nTGVs for the present study.

The doubly off-shell nTGC form factors for  $Z^*\gamma V^*$  vertices are more complicated than the  $Z\gamma V^*$  form factors. Matching with the dimension-8 nTGC operators of the SMEFT, we can parametrize the  $Z^*\gamma V^*$  vertices in terms of the following form factors:

$$V_{Z^*\gamma V^*}^{\alpha\beta\mu} = \Gamma_{Z^*\gamma V^*}^{\alpha\beta\mu} + \frac{e}{M_Z^2} q_1^\alpha X_{1V}^{\beta\mu} + \frac{e}{M_Z^2} q_3^\mu X_{3V}^{\alpha\beta}, \quad (2.4)$$

where expressions for  $X_{1V}^{\beta\mu}$  and  $X_{3V}^{\alpha\beta}$  are given in Appendix A and we find that they make vanishing contributions to the reaction  $f\bar{f} \rightarrow Z^{(*)}\gamma$  with  $Z^{(*)} \rightarrow f'f'$ . Hence, the present analysis only involves the vertices  $\Gamma_{Z^*\gamma V^*}^{\alpha\beta\mu}$ .

We present first the CPC parts of the  $\Gamma_{Z^*\gamma V^*}^{\alpha\beta\mu}$  vertices:

$$\Gamma_{Z^*\gamma\gamma^*}^{\alpha\beta\mu}(q_1, q_2, q_3) = \frac{e}{M_Z^2} \left( h_{31}^\gamma + \frac{\hat{h}_3^\gamma q_1^2}{M_Z^2} \right) q_3^2 q_{2\nu} \epsilon^{\alpha\beta\mu\nu} + \frac{e s_W \hat{h}_4 q_3^2}{2 c_W M_Z^4} (2 q_2^\alpha q_{3\nu} q_{2\sigma} \epsilon^{\beta\mu\nu\sigma} + q_3^2 q_{2\nu} \epsilon^{\alpha\beta\mu\nu}), \quad (2.5a)$$

$$\Gamma_{Z^*\gamma Z^*}^{\alpha\beta\mu}(q_1, q_2, q_3) = \frac{e(q_3^2 - q_1^2)}{M_Z^2} \left[ \hat{h}_3^Z q_{2\nu} \epsilon^{\alpha\beta\mu\nu} + \frac{\hat{h}_4}{2 M_Z^2} (2 q_2^\alpha q_{3\nu} q_{2\sigma} \epsilon^{\beta\mu\nu\sigma} + q_3^2 q_{2\nu} \epsilon^{\alpha\beta\mu\nu}) \right]. \quad (2.5b)$$

In the above, we use the hat symbol to distinguish off-shell form factors ( $\hat{h}_3^Z, \hat{h}_3^\gamma, \hat{h}_4$ ) from their on-shell counterparts ( $h_3^Z, h_3^\gamma, h_4$ ) as studied in [1]. The CPC form-factor parameters ( $h_{31}^\gamma, \hat{h}_3^\gamma, \hat{h}_3^Z, \hat{h}_4$ ) can be mapped precisely to the cutoff scales ( $\Lambda_{\widetilde{BW}}, \Lambda_{\widetilde{BW}}, \Lambda_{G-}, \Lambda_{G+}$ ) of the dimension-8 operators ( $\mathcal{O}_{\widetilde{BW}}, \mathcal{O}_{\widetilde{BW}}, \mathcal{O}_{G+}, \mathcal{O}_{G-}$ ), as follows:

$$\hat{h}_4 = \frac{\hat{r}_4}{[\Lambda_{G+}^4]}, \quad \hat{h}_3^Z = \frac{\hat{r}_3^Z}{[\Lambda_{\widetilde{BW}}^4]}, \quad \hat{h}_3^\gamma = \frac{\hat{r}_3^\gamma}{[\Lambda_{G-}^4]}, \quad h_{31}^\gamma = \frac{r_{31}^\gamma}{[\Lambda_{\widetilde{BW}}^4]}, \quad (2.6a)$$

$$\hat{r}_4 = -\frac{v^2 M_Z^2}{s_W c_W}, \quad \hat{r}_3^Z = \frac{v^2 M_Z^2}{2 s_W c_W}, \quad \hat{r}_3^\gamma = -\frac{v^2 M_Z^2}{2 c_W^2}, \quad r_{31}^\gamma = -\frac{v^2 M_Z^2}{s_W c_W}, \quad (2.6b)$$

where  $[\Lambda_j^4] \equiv \text{sign}(\tilde{c}_j) \Lambda_j^4$ . The above relations hold for any momentum  $q_1$  of  $Z^*$ , and for  $q_1^2 = M_Z^2$  the off-shell form factors ( $\hat{h}_3^Z, \hat{h}_3^\gamma, \hat{h}_4$ ) reduce to the on-shell cases,  $\hat{h}_4 = h_4$ ,  $\hat{h}_3^Z = h_3^Z$ , and  $\hat{h}_3^\gamma + h_{31}^\gamma = h_3^\gamma$ , where  $h_{31}^\gamma$  is part of the on-shell form factor,  $h_{31}^\gamma = h_3^\gamma - \hat{h}_3^\gamma$ , for  $q_1^2 = M_Z^2$ .

We note that the formulations of the off-shell nTGC form factors  $Z^*\gamma V^*$  in Eq.(2.5) (the CPC case) and in Eq.(2.7) (the CPV case) were not given explicitly in the previous literature, including Refs. [7]-[8]. As we discuss in Section 3, CMS [4] and ATLAS [5] both measured the CPC nTGC form factors  $h_3^\gamma$  and  $h_4^V$  via the reaction  $pp(q\bar{q}) \rightarrow Z^*\gamma \rightarrow \nu\bar{\nu}\gamma$ , but both used the conventional CPC nTGC form factor formulation of  $Z\gamma V^*$  in which both the final-state bosons  $Z, \gamma$  are assumed to be on-shell [7]. Hence their measurement of  $h_3^\gamma$  is simply equivalent to measuring the form factor  $h_{31}^\gamma$  in Eq.(2.5a) above [13]. Therefore the CMS and ATLAS analyses [4][5] missed the new form factor  $\hat{h}_3^\gamma$  in Eq.(2.5a), whose contribution dominates over that of  $h_{31}^\gamma$  in the  $\nu\bar{\nu}\gamma$  channel for both the LHC and 100TeV  $pp$  colliders, as we demonstrate in Section 3.

Next, using the Lagrangian (A.3) for nTGVs, we construct the following off-shell CPV nTGVs  $\Gamma_{Z^*\gamma V^*}^{\alpha\beta\mu}$ :

$$\Gamma_{Z^*\gamma\gamma^*}^{\alpha\beta\mu}(q_1, q_2, q_3) = \frac{e}{M_Z^2} \left( h_{11}^\gamma + \frac{\hat{h}_1^\gamma q_1^2}{M_Z^2} \right) q_3^2 (q_2^\alpha g^{\mu\beta} - q_2^\mu g^{\alpha\beta}) + \frac{e s_W \hat{h}_2 q_3^2}{2 c_W M_Z^4} (q_1^2 q_2^\alpha g^{\mu\beta} - q_3^2 q_2^\mu g^{\alpha\beta}), \quad (2.7a)$$

$$\Gamma_{Z^*\gamma Z^*}^{\alpha\beta\mu}(q_1, q_2, q_3) = \frac{e(q_3^2 - q_1^2)}{M_Z^2} \left[ \hat{h}_1^Z (q_2^\alpha g^{\mu\beta} - q_2^\mu g^{\alpha\beta}) + \frac{\hat{h}_2}{2 M_Z^2} (q_1^2 q_2^\alpha g^{\mu\beta} - q_3^2 q_2^\mu g^{\alpha\beta}) \right], \quad (2.7b)$$

which have important differences from the conventional CPV nTGC form factors [7] as we explain in Appendix A. We note that when the final-state  $Z$  boson is on-shell ( $q_1^2 = M_Z^2$ ), the above off-shell form factors should reduce to the on-shell ones,  $h_{11}^\gamma + \hat{h}_1^\gamma = h_1^\gamma$ ,  $\hat{h}_1^Z = h_1^Z$ , and  $\hat{h}_2 = h_2$ . In the on-shell limit, the longitudinally polarized on-shell external state  $Z_L(q_1)$  should

satisfy the equivalence theorem (ET) [14], which puts nontrivial constraints on the structure of form factors, as shown in Appendix A.

Then, we can match these CPV nTGC form factors to the dimension-8 gauge-invariant CPV operators (2.2)-(2.3) in the broken phase and derive the following correspondence relations:

$$\hat{h}_1^Z = v^2 M_Z^2 \left( -\frac{1}{4[\Lambda_{WW}^4]} + \frac{c_W^2 - s_W^2}{4c_W s_W [\Lambda_{WB}^4]} + \frac{1}{[\Lambda_{BB}^4]} \right), \quad (2.8a)$$

$$h_{11}^\gamma = v^2 M_Z^2 \left( -\frac{s_W}{4c_W [\Lambda_{WW}^4]} + \frac{1}{2[\Lambda_{WB}^4]} - \frac{c_W}{s_W [\Lambda_{BB}^4]} \right), \quad (2.8b)$$

$$\hat{h}_1^\gamma = \frac{v^2 M_Z^2}{4c_W^2 [\Lambda_{G-}^4]}, \quad (2.8c)$$

$$\hat{h}_2 = -\frac{v^2 M_Z^2}{2s_W c_W [\Lambda_{G+}^4]}. \quad (2.8d)$$

We find that the CPV operators (2.2d)-(2.2e) that contain Higgs fields can generate the form factors  $(h_{11}^\gamma, h_1^Z)$ , where  $h_{11}^\gamma$  is part of the on-shell form factor  $h_1^\gamma = h_{11}^\gamma + \hat{h}_1^\gamma$ .

In summary, there are eight independent CPC and CPV form factors for the nTGC vertices  $Z^* \gamma V^*$ . These can be mapped to the four CPC operators (2.2a)-(2.2b), (2.3a)-(2.3b) and the five CPV operators (2.2c)-(2.2e), (2.3c)-(2.3d). In the case of  $Z \gamma V^*$  vertices with on-shell  $Z$  and  $\gamma$ , there are only six independent parameters because  $h_{31}^\gamma + \hat{h}_3^\gamma = h_3^\gamma$  and  $h_{11}^\gamma + \hat{h}_1^\gamma = h_1^\gamma$ . Matching the nTGC form factors with the corresponding dimension-8 operators of the SMEFT, we observe that the  $(h_{11}^\gamma, h_{31}^\gamma)$  and  $(\hat{h}_1^Z, \hat{h}_3^Z)$  form factors arise as a consequence of spontaneous electroweak symmetry breaking, and would vanish if  $\langle H \rangle = 0$ . We also note that  $\hat{h}_{1,3}^\gamma$  and  $\hat{h}_{2,4}$  arise from the electroweak rotation of the  $BW^3W^3$  vertex, so the  $\hat{h}_1^\gamma$  term in Eq.(2.7a) and  $\hat{h}_3^\gamma$  term in Eq.(2.5a) would vanish if  $s_W = 0$ .

In passing, we have also derived the perturbative unitarity bounds on the cutoff scales  $\Lambda_j$  and the form factors  $h_j^V$  in Appendix C. We verify that these bounds are much weaker than our current collider bounds (presented in Sec. 3) and thus do not affect our collider analyses.

### 3 Probing nTGCs with $Z^* \gamma (\nu \bar{\nu} \gamma)$ Production at Hadron Colliders

The invariant mass of  $Z^{(*)} \rightarrow \nu \bar{\nu}$  decays cannot be measured in the reaction  $pp(q\bar{q}) \rightarrow \nu \bar{\nu} \gamma$  at hadron colliders, so it becomes impossible to determine whether the invisible  $Z$ -decay is on-shell or not. Hence analyzing the  $\nu \bar{\nu} \gamma$  production with off-shell  $Z^*$  decays is important for hadron colliders.

The cross section for  $q\bar{q} \rightarrow Z^{(*)} \gamma$  at a  $pp$  collider can be expressed as

$$\sigma = \sum_{q, \bar{q}} \int dx_1 dx_2 [\mathcal{F}_{q/p}(x_1, \mu) \mathcal{F}_{\bar{q}/p}(x_2, \mu) \sigma_{q\bar{q}}(\hat{s}) + (q \leftrightarrow \bar{q})], \quad (3.1)$$

where the functions  $\mathcal{F}_{q/p}$  and  $\mathcal{F}_{\bar{q}/p}$  are the parton distribution functions (PDFs) of the quark and antiquark in the proton beams, and  $\hat{s} = x_1 x_2 s$ . The PDFs depend on the factorization scale  $\mu$ , which we set to  $\mu = \sqrt{\hat{s}}/2$  in our leading-order analysis. We use the PDFs of the quarks  $q = u, d, s, c, b$  and their antiquarks determined by the CTEQ collaboration [15]. In principle,  $\hat{s}$  can be determined by measuring the invariant-mass of observable final-state particles. ATLAS

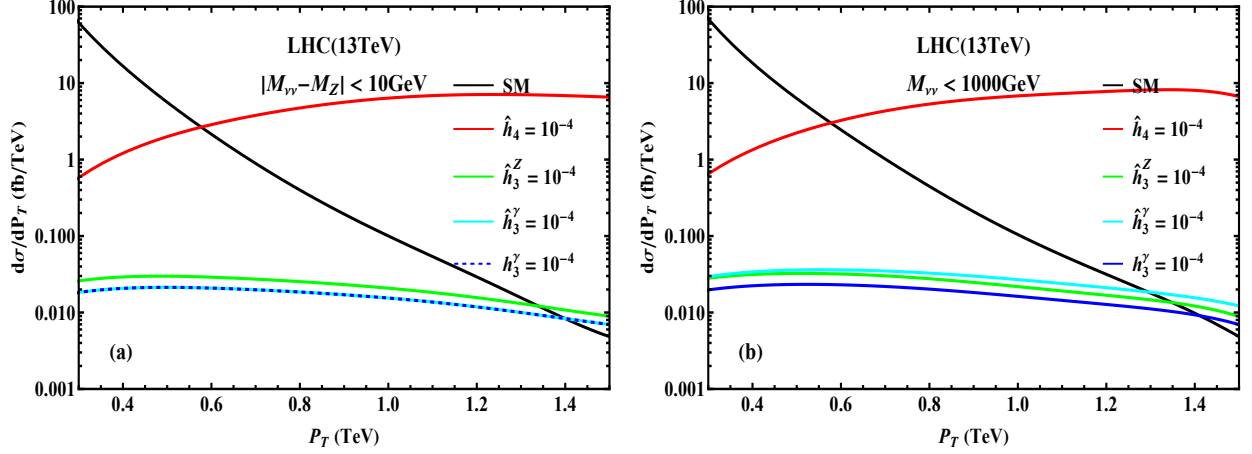


Figure 1: Differential cross sections for  $\nu\bar{\nu}\gamma$  production as functions of the photon transverse momentum  $P_T^\gamma$ , shown in plot (a) for the LHC(13TeV) and in plot (b) for the projected 100TeV  $pp$  collider. In each plot, the SM cross section is given by a black curve, and the contributions of the different nTGC form factors (for a reference value  $10^{-4}$ ) are shown by the colored curves.

measurements of  $M_{\ell\ell\gamma}$  during the LHC Run-2 reached around 3 TeV. Accordingly, in our analysis of  $Z^*\gamma(\nu\bar{\nu}\gamma)$  production we consider the relevant range  $\hat{s} < 3$  TeV for the LHC and  $\hat{s} < 23$  TeV for a 100TeV  $pp$  collider.

We compute the partonic cross-section in three parts,

$$\sigma(q\bar{q} \rightarrow Z^*\gamma) = \sigma_0 + \sigma_1 + \sigma_2, \quad (3.2)$$

where  $\sigma_0$  is the SM contribution,  $\sigma_1$  is the contribution of the nTGCs interfering with the SM amplitude, and  $\sigma_2$  denotes the squared nTGC contribution. We present explicit formulae for  $(\sigma_0, \sigma_1, \sigma_2)$  in Appendix B. The CPC and CPV amplitudes do not interfere for  $q\bar{q} \rightarrow Z^{(*)}\gamma$ , hence the contributions of the CPV nTGCs to  $\sigma_1$  vanish. Moreover, we find that  $\sigma_1 \ll \sigma_2$  holds for the CPC nTGCs at the LHC and future  $pp$  colliders, making  $\sigma_1$  negligible in this analysis [16]. We further observe that each CPV nTGC gives the same contribution to  $\sigma_2$  as that of the corresponding CPC nTGC.

The final state  $\gamma$  is the only visible particle when  $Z^{(*)}$  has invisible decays, and the longitudinal momentum of the  $\nu\bar{\nu}$  pair cannot be measured at hadron colliders. Hence, the photon's transverse momentum  $P_T^\gamma$  is the main variable that can be used to distinguish the new physics signals from the SM backgrounds. We present in Fig. 1 distributions of the  $Z^*\gamma$  cross section for the LHC (13TeV) in plot (a) and for the projected 100 TeV  $pp$  collider in plot (b). In each plot, the SM cross section is given by the black curve, and the contributions of the nTGC form factors ( $\hat{h}_4, \hat{h}_3^Z, \hat{h}_3^\gamma, h_{31}^\gamma$ ) (taking a reference value  $10^{-4}$ ) are shown by the blue, green, red and red-dashed curves. We observe from Eq.(2.5a) that the  $\hat{h}_3^\gamma$  contribution is strongly enhanced by the off-shell  $Z^*$  momentum factor  $q_1^2/M_Z^2$ , whereas the  $\hat{h}_{31}^\gamma$  contribution is not. Unlike  $\hat{h}_3^\gamma$ , this does not happen to  $\hat{h}_3^Z$  because Eq.(2.5b) shows that the numerator factor  $q_3^2 - q_1^2$  exhibits a strong cancellation between  $q_3^2 (= \hat{s})$  and  $q_1^2$  when  $q_1^2$  goes far off-shell, which is particularly relevant for the high-energy 100 TeV  $pp$  collider. We find that the  $\hat{h}_3^\gamma$  contribution (red solid curve) is larger than that of  $\hat{h}_{31}^\gamma$  (red dashed curve) by about (50–60)% for the LHC, as seen in Fig. 1(a), and by a larger factor of (40–70) in the case of the 100 TeV  $pp$  collider, as seen in Fig. 1(b). We note that the  $\hat{h}_4$  contribution is much larger than that of  $\hat{h}_3^Z$ ,  $\hat{h}_3^\gamma$ , and  $h_{31}^\gamma$ , because the  $\hat{h}_4$  terms are enhanced by an extra large momentum factor of  $q_2q_3$  or  $q_3^2$ , as shown



$\sqrt{s}$	13 TeV				100 TeV		
$\mathcal{L}(\text{ab}^{-1})$	0.14	0.3	3		3	10	30
$ \hat{h}_{4,2}  \times 10^6$	11	8.5	4.2	$ \hat{h}_{4,2}  \times 10^9$	4.5	2.9	2.0
$ \hat{h}_{3,1}^Z  \times 10^4$	2.2	1.7	0.90	$ \hat{h}_{3,1}^Z  \times 10^7$	7.0	4.8	3.4
$ \hat{h}_{3,1}^\gamma  \times 10^4$	1.6	1.3	0.67	$ \hat{h}_{3,1}^\gamma  \times 10^7$	0.94	0.62	0.44
$ h_{31,11}^\gamma  \times 10^4$	2.5	2.0	1.0	$ h_{31,11}^\gamma  \times 10^7$	8.3	5.7	4.0

Table 1: Sensitivity reaches on probing the CPC and CPV nTGC form factors at the  $2\sigma$  level, as obtained by analyzing the reaction  $pp(q\bar{q}) \rightarrow Z^*\gamma \rightarrow \nu\bar{\nu}\gamma$  at the LHC (13 TeV) and the 100 TeV  $pp$  collider, for the indicated integrated luminosities. In the last two rows, the  $\hat{h}_{3,1}^\gamma$  sensitivities (red color) include the  $Z^*$ -momentum-square ( $q_1^2$ ) enhanced off-shell effects, whereas the  $h_{31,11}^\gamma$  sensitivities (blue color) do not.

in Eq.(2.5).

In order to optimize the detection sensitivity, we divide events into bins of the  $P_T(\gamma)$  distribution, whose widths we take as  $\Delta P_T = 100$  GeV for the LHC and  $\Delta P_T = 500$  GeV for the 100 TeV  $pp$  collider. Then, we compute the significance  $\mathcal{Z}_{\text{bin}}$  for each bin, and construct the following total significance measure:

$$\mathcal{Z}_{\text{total}} = \sqrt{\sum \mathcal{Z}_{\text{bin}}^2}. \quad (3.3)$$

Since the SM contribution  $\sigma_0$  becomes small when the photon  $P_T$  is high, we determine the statistical significance by using the following formula for the background-with-signal hypothesis [20]:

$$\mathcal{Z} = \sqrt{2 \left( B \ln \frac{B}{B+S} + S \right)} = \sqrt{2 \left( \sigma_0 \ln \frac{\sigma_0}{\sigma_0 + \Delta\sigma} + \Delta\sigma \right)} \times \sqrt{\mathcal{L} \times \epsilon}, \quad (3.4)$$

where  $\mathcal{L}$  is the integrated luminosity and  $\epsilon$  denotes the detection efficiency. For our analysis we choose an ideal detection efficiency  $\epsilon = 100\%$  unless specified otherwise.

We present sensitivities for probing the CPC and CPV nTGC form factors and the corresponding new physics scales of the dimension-8 nTGC operators in Tables 1 and 2, respectively. For the LHC, we find that the sensitivities to  $\hat{h}_2$  and  $\hat{h}_4$  can reach the level of  $O(10^{-5} - 10^{-6})$ , whereas the sensitivities to  $\hat{h}_{3,1}^Z$ ,  $\hat{h}_{3,1}^\gamma$  and  $h_{31,11}^\gamma$  are of  $O(10^{-4})$ . The sensitivities for probing the nTGC form factors at the projected 100 TeV  $pp$  collider are generally much higher than those at the LHC, by a factor of  $O(10^2 - 10^3)$ . At the LHC the sensitivities to  $\hat{h}_{3,1}^\gamma$  are stronger than those to  $h_{31,11}^\gamma$  and  $\hat{h}_{3,1}^Z$  by about (50–60)%, whereas at the 100 TeV  $pp$  collider the sensitivities to  $\hat{h}_{3,1}^\gamma$  are much higher than those to  $h_{31,11}^\gamma$  and  $\hat{h}_{3,1}^Z$ , by factors of  $O(10)$ .

We recall that both CMS (using 19.6/fb of Run-1 data) [4] and ATLAS (using 36.9/fb of Run-2 data) [5] measured the CPC nTGC form factors ( $h_3^V$ ,  $h_4^V$ ) via the reaction  $pp(q\bar{q}) \rightarrow Z^*\gamma \rightarrow \nu\bar{\nu}\gamma$ ; but they used the conventional CPC nTGC form factor formulation of the  $Z\gamma V^*$  vertex with both  $Z\gamma$  being on-shell [7]. This differs from our off-shell formulation of the  $Z^*\gamma V^*$  vertex in Eq.(2.5), which gives the correct nTGC form factor formulation for analyzing the reaction  $pp(q\bar{q}) \rightarrow Z^*\gamma \rightarrow \nu\bar{\nu}\gamma$  at hadron colliders. For instance, using 36.1/fb of Run-2 data at

$\sqrt{s}$	13 TeV			100 TeV		
$\mathcal{L} \text{ (ab}^{-1}\text{)}$	0.14	0.3	3	3	10	30
$\Lambda_{G+}(\text{CPC})$	3.2	3.5	4.1	23	25	28
$\Lambda_{G-}(\text{CPC})$	1.2	1.3	1.5	7.7	8.5	9.3
$\Lambda_{\widetilde{BW}}(\text{CPC})$	1.3	1.4	1.6	5.4	5.9	6.4
$\Lambda_{\widetilde{BW}}(\text{CPC})$	1.5	1.6	1.8	6.2	6.8	7.4
$\Lambda_{\widetilde{G}+}(\text{CPV})$	2.7	2.9	3.5	19	21	23
$\Lambda_{\widetilde{G}-}(\text{CPV})$	1.0	1.1	1.3	6.5	7.2	7.8
$\Lambda_{WW}(\text{CPV})$	0.93	0.98	1.2	3.9	4.3	4.6
$\Lambda_{WB}(\text{CPV})$	1.1	1.2	1.4	4.6	5.1	5.5
$\Lambda_{BB}(\text{CPV})$	1.3	1.4	1.7	5.6	6.2	6.8

Table 2: Sensitivity reaches on probing the new physics scales  $\Lambda_j$  (TeV) of the dimension-8 nTGC operators at  $2\sigma$  level, as derived by analyzing the reaction  $pp(q\bar{q}) \rightarrow Z^* \gamma \rightarrow \nu \bar{\nu} \gamma$  at the LHC (13 TeV) and at a 100 TeV  $pp$  collider, with the integrated luminosities  $\mathcal{L}$  as shown in this table.

the LHC(13 TeV), ATLAS obtained the following bounds at 95% C.L. [5]:

$$\begin{aligned} h_3^\gamma &\in (-3.7, 3.7) \times 10^{-4}, & h_3^Z &\in (-3.2, 3.3) \times 10^{-4}, \\ h_4^\gamma &\in (-4.4, 4.3) \times 10^{-7}, & h_4^Z &\in (-4.5, 4.4) \times 10^{-7}. \end{aligned} \quad (3.5)$$

For a quantitative comparison, we impose the same cut  $P_T^\gamma > 600$  GeV as that of the ATLAS analysis [5] and choose a detection efficiency  $\epsilon = 70\%$  [5][19]. We then derive the following LHC bounds on the CPC nTGCs at 95% C.L.:

$$|h_{31}^\gamma| < 3.5 \times 10^{-4}, \quad |\hat{h}_3^\gamma| < 2.3 \times 10^{-4}, \quad |\hat{h}_3^Z| < 3.1 \times 10^{-4}, \quad |\hat{h}_4| < 1.4 \times 10^{-5}. \quad (3.6)$$

Comparing our results (3.6) with the ATLAS result (3.5), we find that our bounds on  $h_{31}^\gamma$  and  $\hat{h}_3^Z$  agree well with the ATLAS bounds on  $h_3^\gamma$  and  $h_3^Z$  (to within a few percent), whereas our bound on  $\hat{h}_3^\gamma$  is significantly stronger than the ATLAS bound on  $h_3^\gamma$  by about 60%. This is because in our off-shell formulation of Eq.(2.5) the form factor  $\hat{h}_3^\gamma$  is enhanced by the  $Z^*$  off-shell factor  $q_1^2/M_Z^2$ , but  $h_{31}^\gamma$  and  $\hat{h}_3^Z$  are not and thus their bounds are quite similar to the case of assuming on-shell invisible  $Z$  decays. On the other hand, our  $\hat{h}_4$  bound in Eq.(3.6) is much weaker than the ATLAS bounds on  $(h_4^\gamma, h_4^Z)$ , by a factor of  $\sim 30$ , because the conventional nTGC form factor formulae are incompatible with the gauge-invariant SMEFT formulation of dimension-8 (including spontaneous electroweak gauge symmetry breaking), as we explain in Appendix A and Table 3. We emphasize that the existing ATLAS result [5] used the conventional on-shell nTGC formula of the vertex  $Z\gamma V^*$  [7] for analyzing the  $\nu\bar{\nu}\gamma$  channel, which caused a significant underestimate of the sensitivity to  $\hat{h}_3^\gamma$  by about 60%. This underlines the importance for the on-going LHC experimental analyses to use *the correct theoretical formalism* to analyze the  $\nu\bar{\nu}\gamma$  channel for probing the nTGCs, as proposed in this work.

In Table 2 we demonstrate that the sensitivities to new physics scales in the coefficients of  $\mathcal{O}_{G+}$  and  $\widetilde{\mathcal{O}}_{G+}$  can reach  $(2.7 - 4.1)$  TeV at the LHC, and  $(19 - 28)$  TeV at the 100 TeV  $pp$  collider. The sensitivities to probing new physics scales of other nTGC operators are around



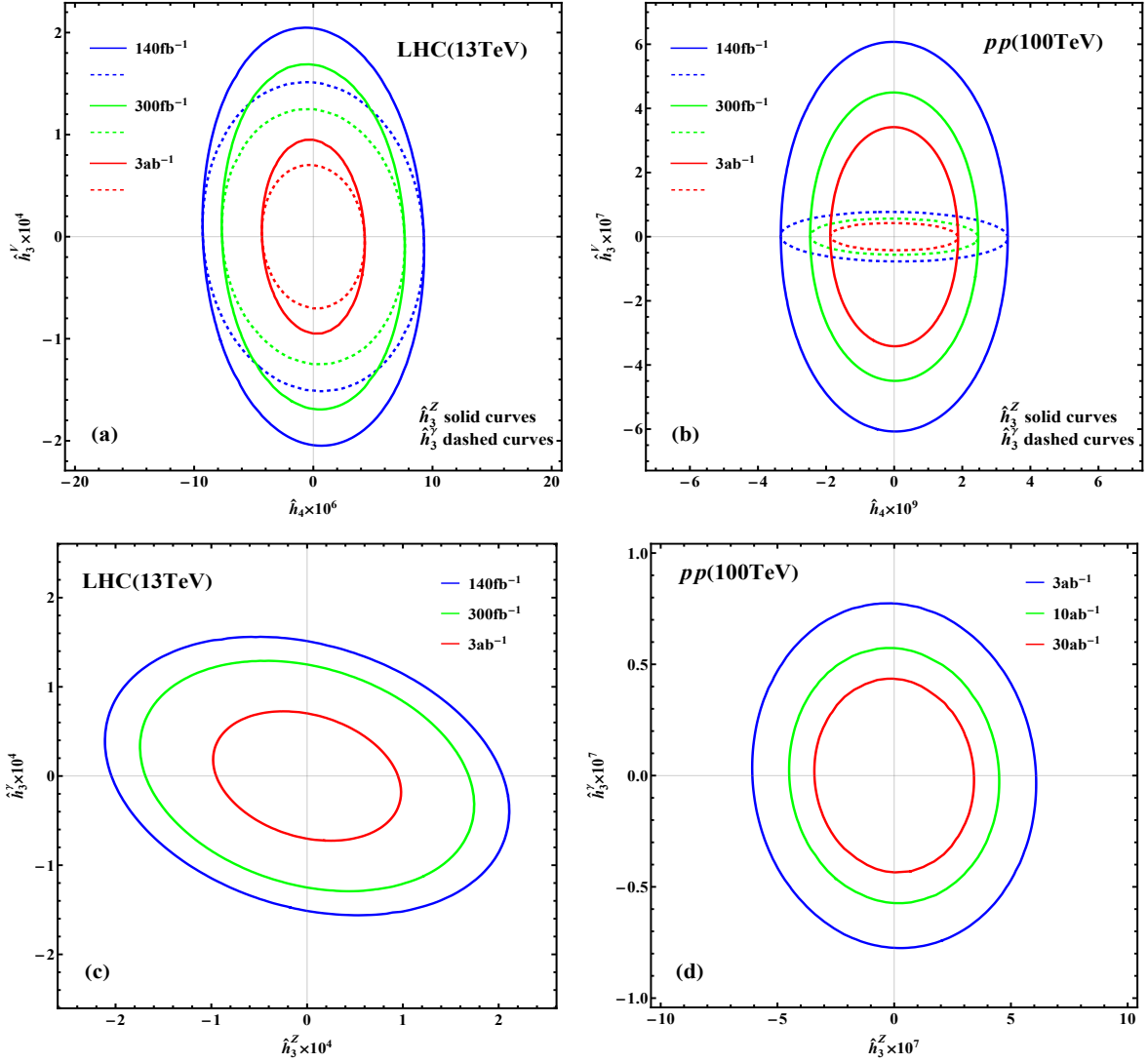


Figure 2: Correlation contours (95% C.L.) for the sensitivities to each pairs of nTGC form factors at the LHC(13 TeV) [panels (a) and (c)] and the 100 TeV  $pp$  collider [panels (b) and (d)]. Panels (a) and (b) show the correlation contours for  $(h_4, h_3^Z)$  (solid curves) and  $(h_4, h_3^\gamma)$  (dashed curves), and panels (c) and (d) depict the correlation contours for  $(h_3^Z, h_3^\gamma)$ .

(1 – 1.8) TeV at the LHC and (3.9 – 9.3) TeV at the 100 TeV  $pp$  collider. We find that the sensitivities to the coefficients of  $\mathcal{O}_{G-}$ ,  $\widetilde{\mathcal{O}}_{G-}$  and  $\hat{h}_{1,3}^\gamma$  are significantly higher than that of the case by assuming the on-shell  $Z\gamma$  final states [1].

Finally, we analyze the correlation contours (95% C.L.) between the sensitivities to the form factors of the off-shell nTGC vertex  $Z^*\gamma V^*$ , as shown in Fig. 2, where we have chosen an ideal detection efficiency  $\epsilon=100\%$ . We find that the behavior of the  $\hat{h}_4 - \hat{h}_3^Z$  correlation is similar to that of their on-shell counterparts  $h_4$  and  $h_3^Z$  [1]. Specifically, the  $\hat{h}_4 - \hat{h}_3^V$  correlation is rather small, while the sensitivity to  $\hat{h}_3^\gamma$  is much greater than that to  $h_{31}^\gamma$ , especially at a 100 TeV  $pp$  collider. On the other hand, the correlation between  $\hat{h}_3^Z - \hat{h}_3^\gamma$  is large at the LHC, but small at a 100 TeV  $pp$  collider. This is because at the LHC the contributions of both  $\hat{h}_3^Z$  and  $\hat{h}_3^\gamma$  contain large portions of on-shell effects which are comparable, whereas at the 100 TeV  $pp$  collider the  $\hat{h}_3^Z$  contribution is still dominated by the on-shell effect, but the off-shell effects are highly enhanced and dominate the  $\hat{h}_3^\gamma$  contribution.

We note that the CPC and CPV nTGCs have no correlations because their amplitudes only differ by  $\pm i$ . Finally, correlations between  $\hat{h}_2$ ,  $\hat{h}_1^Z$ ,  $\hat{h}_1^\gamma$  and  $h_{11}^\gamma$  are similar to those of the corresponding CPC nTGCs, because the squared term  $\sigma_2$  dominates the signal cross section at the LHC and the 100 TeV  $pp$  collider.

## 4 Conclusions

In this work, we have demonstrated that the reaction  $pp(q\bar{q}) \rightarrow Z^*\gamma \rightarrow \nu\bar{\nu}\gamma$  can probe sensitively both the CPC and CPV nTGCs at the LHC and at the projected 100 TeV  $pp$  colliders. It has comparable sensitivities to the on-shell production channels  $pp(q\bar{q}) \rightarrow Z\gamma$  with  $Z \rightarrow \ell^+\ell^-$  [1]. Because the on-shell constraint cannot be imposed on the final state  $Z$  boson with invisible decays at hadron colliders, we studied the  $Z^*\gamma$  production with off-shell decays  $Z^* \rightarrow \nu\bar{\nu}$ . For this, we presented a new general formulation of the CPC/CPV doubly off-shell  $Z^*\gamma V^*$  form factors and their nontrivial matching with the full  $SU(2) \otimes U(1)$  gauge-invariant SMEFT operators of dimension-8. In consequence, we found that the conventional on-shell form factors for  $Z\gamma V^*$  vertices [7] are inadequate, and the conventional form factors  $(h_3^V, h_4^V)$  and  $(h_1^V, h_2^V)$  must be replaced by two sets of new form factors  $(h_{31}^\gamma, \hat{h}_3^V, \hat{h}_4)$  and  $(h_{11}^\gamma, \hat{h}_1^V, \hat{h}_2)$ , as shown in Eqs.(2.5) and (2.7).

In the  $\nu\bar{\nu}\gamma$  production channel at  $pp$  colliders, only the photon  $P_T^\gamma$  is measurable, and we have studied how to optimize the sensitivities to nTGCs by proper choices of  $P_T^\gamma$  bins at the LHC and the projected 100 TeV  $pp$  colliders. Since the interference cross section is always negligible relative to the squared term at these colliders [16], the sensitivities to the CPV nTGCs are similar to those to the corresponding CPC nTGCs.

We have presented the prospective sensitivity reaches on the nTGC form factors  $\hat{h}_j^V$  (compatible with the full electroweak gauge symmetry with spontaneous breaking) at the LHC and the 100 TeV  $pp$  collider in Table 1, and the sensitivity reaches on probing the new physics scales  $\Lambda_j$  of the corresponding dimension-8 nTGC operators in Table 2. We found in Table 1 that including the off-shell decays  $Z^* \rightarrow \nu\bar{\nu}$  can increase the sensitivity reaches for  $(\hat{h}_3^\gamma, \hat{h}_1^\gamma)$  by (50–60)% at the LHC and by a factor of  $O(10)$  at the 100 TeV  $pp$  collider. We present in Fig. 2 the correlations between the sensitivities to each pair of nTGC form factors.

We further made quantitative comparisons between the existing ATLAS measurements [5] of the CPC nTGC form factors and our theory predictions, as shown in Eqs.(3.5)-(3.6). We found that for the  $\nu\bar{\nu}\gamma$  channel the LHC sensitivity reaches on probing the nTGC form factors  $\hat{h}_3^\gamma$  and  $\hat{h}_4$  differ significantly from the ATLAS results (using the conventional  $Z\gamma V^*$  formulae which are inconsistent with spontaneous breaking of the electroweak gauge symmetry).

This work establishes a new perspective for on-going experimental probes of the new physics in nTGCs at the LHC and the projected 100 TeV  $pp$  colliders. We look forward to continuing the fruitful cooperation with the LHC experimental groups, extending their on-going nTGC analyses by using our new nTGC formulation, which consistently incorporates the nTGC form factors with the corresponding gauge-invariant dimension-8 operators of the SMEFT.

## Acknowledgements

The work of JE was supported in part by United Kingdom STFC Grant ST/T000759/1, and in part by the SJTU distinguished visiting fellow programme. The work of HJH and RQX was supported in part by the National NSF of China (under grants 11835005 and 12175136).

RQX has been supported by an International Postdoctoral Exchange Fellowship.

## Appendix

### A Matching $Z^*\gamma V^*$ Form Factors to the SMEFT Operators

Working in the broken electroweak phase of the SM,  $SU(2)_W \otimes U(1)_Y \rightarrow U(1)_{\text{em}}$ , we expand the CPC operators and derive the relevant neutral triple gauge vertices (nTGVs) as follows:

$$\mathcal{O}_{G+}(\text{CPC}) \rightarrow \frac{ev^2}{4M_Z^2 s_W c_W} (c_W^2 \tilde{A}_{\mu\nu} Z^{\mu\rho} - s_W^2 \tilde{Z}_{\mu\nu} A^{\mu\rho} + c_W s_W \tilde{A}_{\mu\nu} A^{\mu\rho} - c_W s_W \tilde{Z}_{\mu\nu} Z^{\mu\rho}) \partial^2 \left( Z_\rho^\nu + \frac{s_W}{c_W} A_\rho^\nu \right), \quad (\text{A.1a})$$

$$\begin{aligned} \mathcal{O}_{G-}(\text{CPC}) \rightarrow & -\frac{ev^2}{4M_Z^2 s_W c_W} (c_W^2 \tilde{A}_{\mu\nu} Z^{\mu\rho} - s_W^2 \tilde{Z}_{\mu\nu} A^{\mu\rho} + c_W s_W \tilde{A}_{\mu\nu} A^{\mu\rho} - c_W s_W \tilde{Z}_{\mu\nu} Z^{\mu\rho}) \\ & \times \left[ \partial^2 \left( \partial^\nu Z_\rho + \partial_\rho Z^\nu + \frac{s_W}{c_W} \partial^\nu A_\rho + \frac{s_W}{c_W} \partial_\rho A^\nu \right) - 2\partial^\nu \partial_\rho \left( \partial_\alpha Z^\alpha + \frac{s_W}{c_W} \partial_\alpha A^\alpha \right) \right], \end{aligned} \quad (\text{A.1b})$$

$$\mathcal{O}_{\tilde{B}W}(\text{CPC}) \rightarrow \frac{ev^2}{4s_W c_W} (c_W^2 \tilde{A}_{\mu\nu} Z^{\mu\rho} - s_W^2 \tilde{Z}_{\mu\nu} A^{\mu\rho} + c_W s_W \tilde{A}_{\mu\nu} A^{\mu\rho} - c_W s_W \tilde{Z}_{\mu\nu} Z^{\mu\rho}) (\partial^\nu Z_\rho + \partial_\rho Z^\nu), \quad (\text{A.1c})$$

$$\mathcal{O}_{\tilde{B}\tilde{W}}(\text{CPC}) \rightarrow \frac{-ev^2}{2s_W c_W} (\partial_\rho \tilde{Z}_{\mu\nu} Z^{\mu\rho} + \partial_\rho \tilde{A}_{\mu\nu} A^{\mu\rho}) Z^\nu, \quad (\text{A.1d})$$

where we adopt the notations  $\tilde{V}^{\mu\nu} = \epsilon^{\mu\nu\alpha\beta} V_{\alpha\beta}$  and  $V^{\mu\nu} = \partial^\mu V^\nu - \partial^\nu V^\mu$  with  $V = A, Z$ .

We then expand the CPV operators in the broken electroweak phase respecting only the residual SM gauge symmetry  $SU(3)_C \otimes U(1)_{\text{em}}$ . In this way we derive the relevant CPV nTGVs as follows:

$$\tilde{\mathcal{O}}_{G+}(\text{CPV}) \rightarrow \frac{ev^2}{4M_Z^2 s_W c_W} A_{\mu\nu} Z^{\mu\rho} \partial^2 \left( Z_\rho^\nu + \frac{s_W}{c_W} A_\rho^\nu \right), \quad (\text{A.2a})$$

$$\begin{aligned} \tilde{\mathcal{O}}_{G-}(\text{CPV}) \rightarrow & -\frac{ev^2}{4M_Z^2 s_W c_W} [c_{2W} (A_{\mu\nu} Z^{\mu\rho} + Z_{\mu\nu} A^{\mu\rho}) + s_{2W} (A_{\mu\nu} A^{\mu\rho} - Z_{\mu\nu} Z^{\mu\rho})] \\ & \times \left[ \partial^2 \left( \partial^\nu Z_\rho + \frac{s_W}{c_W} \partial^\nu A_\rho \right) - \partial^\nu \partial_\rho (\partial \cdot Z + \frac{s_W}{c_W} \partial \cdot A) \right], \end{aligned} \quad (\text{A.2b})$$

$$\tilde{\mathcal{O}}_{BW}(\text{CPV}) \rightarrow \frac{ev^2}{4s_W c_W} [c_{2W} (A_{\mu\nu} Z^{\mu\rho} + Z_{\mu\nu} A^{\mu\rho}) + s_{2W} (A_{\mu\nu} A^{\mu\rho} - Z_{\mu\nu} Z^{\mu\rho})] \partial^\nu Z_\rho, \quad (\text{A.2c})$$

$$\tilde{\mathcal{O}}_{WW}(\text{CPV}) \rightarrow -\frac{ev^2}{4s_W c_W} [s_W c_W (A_{\mu\nu} Z^{\mu\rho} + Z_{\mu\nu} A^{\mu\rho}) + s_W^2 A_{\mu\nu} A^{\mu\rho} + c_W^2 Z_{\mu\nu} Z^{\mu\rho}] \partial^\nu Z_\rho, \quad (\text{A.2d})$$

$$\tilde{\mathcal{O}}_{BB}(\text{CPV}) \rightarrow -ev^2 \left[ -(A_{\mu\nu} Z^{\mu\rho} + Z_{\mu\nu} A^{\mu\rho}) + \frac{c_W}{s_W} A_{\mu\nu} A^{\mu\rho} + \frac{s_W}{c_W} Z_{\mu\nu} Z^{\mu\rho} \right] \partial^\nu Z_\rho, \quad (\text{A.2e})$$

where we have defined  $(s_{2W}, c_{2W}) \equiv (\sin 2\theta_W, \cos 2\theta_W)$ . We note that in Eq.(A.2b) the factor  $\partial \cdot Z$  vanishes for an on-shell  $Z$  boson, while for an off-shell  $Z^*$  it also leads to vanishing results as long as the vector boson couples to a pair of fermions or gauge bosons with equal mass. The same is true for the factor  $\partial \cdot A$ . Thus, we can drop terms with either  $\partial \cdot Z$  or  $\partial \cdot A$  for the present study.

Our next step is to classify the structures of the nTGVs in the broken electroweak phase that are generated by the above SMEFT operators of dimension-8. The Lagrangian of these

nTGVs in the electroweak broken phase contains the following CPC and CPV nTGC form factors:

$$\begin{aligned}
\mathcal{L}_{\text{nTGC}}^{\text{CPC}} = & \frac{e\hat{h}_3^Z}{2M_Z^2} (c_W^2 \tilde{A}_{\mu\nu} Z^{\mu\rho} - s_W^2 \tilde{Z}_{\mu\nu} A^{\mu\rho} + c_W s_W \tilde{A}_{\mu\nu} A^{\mu\rho} - c_W s_W \tilde{Z}_{\mu\nu} Z^{\mu\rho}) (\partial^\nu Z_\rho + \partial_\rho Z^\nu) \\
& - \frac{e\hat{h}_4}{2M_Z^4} (c_W^2 \tilde{A}_{\mu\nu} Z^{\mu\rho} - s_W^2 \tilde{Z}_{\mu\nu} A^{\mu\rho} + c_W s_W \tilde{A}_{\mu\nu} A^{\mu\rho} - c_W s_W \tilde{Z}_{\mu\nu} Z^{\mu\rho}) \partial^2 \left( Z^\nu{}_\rho + \frac{s_W}{c_W} A^\nu{}_\rho \right) \\
& + \frac{e c_W \hat{h}_3^\gamma}{2s_W M_Z^4} (c_W^2 \tilde{A}_{\mu\nu} Z^{\mu\rho} - s_W^2 \tilde{Z}_{\mu\nu} A^{\mu\rho} + c_W s_W \tilde{A}_{\mu\nu} A^{\mu\rho} - c_W s_W \tilde{Z}_{\mu\nu} Z^{\mu\rho}) \times \\
& \left[ \partial^2 \left( \partial^\nu Z_\rho + \partial_\rho Z^\nu + \frac{s_W}{c_W} \partial^\nu A_\rho + \frac{s_W}{c_W} \partial_\rho A^\nu \right) - 2\partial^\nu \partial_\rho \left( \partial \cdot Z + \frac{s_W}{c_W} \partial \cdot A \right) \right] \\
& + \frac{e h_{31}^\gamma}{2M_Z^2} (\partial_\rho \tilde{Z}_{\mu\nu} Z^{\mu\rho} + \partial_\rho \tilde{A}_{\mu\nu} A^{\mu\rho}) Z^\nu,
\end{aligned} \tag{A.3a}$$

$$\begin{aligned}
\mathcal{L}_{\text{nTGC}}^{\text{CPV}} = & \frac{e\hat{h}_1^Z}{M_Z^2} (A_{\mu\nu} Z^{\mu\rho} + Z_{\mu\nu} A^{\mu\rho}) \partial^\nu Z_\rho + \frac{e h_{11}^\gamma}{M_Z^2} A_{\mu\nu} A^{\mu\rho} \partial^\nu Z_\rho - \frac{e\hat{h}_2}{2M_Z^4} A_{\mu\nu} Z^{\mu\rho} \partial^2 \left( Z^\nu{}_\rho + \frac{s_W}{c_W} A^\nu{}_\rho \right) \\
& - \frac{e\hat{h}_1^\gamma}{M_Z^4} \left[ c_{2W} (A_{\mu\nu} Z^{\mu\rho} + Z_{\mu\nu} A^{\mu\rho}) + s_{2W} (A_{\mu\nu} A^{\mu\rho} - Z_{\mu\nu} Z^{\mu\rho}) \right] \\
& \times \left[ \partial^2 \partial^\nu \left( \frac{c_W}{s_W} Z_\rho + A_\rho \right) - \partial^\nu \partial_\rho \partial \cdot \left( \frac{c_W}{s_W} Z + A \right) \right].
\end{aligned} \tag{A.3b}$$

Matching the above form factor Lagrangian with the corresponding dimension-8 nTGC operators in Eq.(A.2), we derive the following relations for the CPC nTGC form factors:

$$\hat{h}_4 = \frac{\hat{r}_4}{[\Lambda_{G+}^4]}, \quad \hat{h}_3^Z = \frac{\hat{r}_3^Z}{[\Lambda_{BW}^4]}, \quad \hat{h}_3^\gamma = \frac{\hat{r}_3^\gamma}{[\Lambda_{G-}^4]}, \quad h_{31}^\gamma = \frac{r_{31}^\gamma}{[\Lambda_{BW}^4]}, \tag{A.4a}$$

$$\hat{r}_4 = -\frac{v^2 M_Z^2}{s_W c_W}, \quad \hat{r}_3^Z = \frac{v^2 M_Z^2}{2s_W c_W}, \quad \hat{r}_3^\gamma = -\frac{v^2 M_Z^2}{2c_W^2}, \quad r_{31}^\gamma = -\frac{v^2 M_Z^2}{s_W c_W}, \tag{A.4b}$$

and for the CPV form factors:

$$\hat{h}_1^Z = v^2 M_Z^2 \left( -\frac{1}{4[\Lambda_{WW}^4]} + \frac{c_W^2 - s_W^2}{4c_W s_W [\Lambda_{WB}^4]} + \frac{1}{[\Lambda_{BB}^4]} \right), \tag{A.5a}$$

$$h_{11}^\gamma = v^2 M_Z^2 \left( -\frac{s_W}{4c_W [\Lambda_{WW}^4]} + \frac{1}{2[\Lambda_{WB}^4]} - \frac{c_W}{s_W [\Lambda_{BB}^4]} \right), \tag{A.5b}$$

$$\hat{h}_1^\gamma = \frac{v^2 M_Z^2}{4c_W^2 [\Lambda_{G-}^4]}, \tag{A.5c}$$

$$\hat{h}_2 = -\frac{v^2 M_Z^2}{2s_W c_W [\Lambda_{G+}^4]}, \tag{A.5d}$$

where  $[\Lambda_j^4] \equiv \text{sign}(\tilde{c}_j) \Lambda_j^4$ . We note that the above relations generally hold at the Lagrangian level.

Next, using the general Lagrangian formulation of nTGVs in Eq.(A.3), we further derive the neutral triple gauge vertices  $Z^* \gamma V^*$  by requiring one photon field  $A^\mu$  be on-shell, where the on-shell photon field satisfies the conditions  $\partial^2 A^\mu = 0$  and  $\partial_\mu A^\mu = 0$ . Thus, we can derive the complete form factor formulation of the neutral triple gauge vertices in momentum space:

$$V_{Z^* \gamma V^*}^{\alpha\beta\mu} = \Gamma_{Z^* \gamma V^*}^{\alpha\beta\mu} + \frac{e}{M_Z^2} X_{1V}^{\beta\mu} q_1^\alpha + \frac{e}{M_Z^2} X_{3V}^{\alpha\beta} q_3^\mu, \tag{A.6}$$

where the expressions of  $X_{1V}^{\beta\mu}$  and  $X_{3V}^{\alpha\beta}$  are given as follows:

$$X_{1V}^{\beta\mu} = \epsilon^{\beta\mu\nu\sigma} q_{2\nu} q_{3\sigma} \left( \chi_{10}^V + \chi_{11}^V \frac{q_1^2}{M_Z^2} + \chi_{13}^V \frac{q_3^2}{M_Z^2} \right) + (q_3^2 - q_1^2) g^{\beta\mu} \left( \tilde{\chi}_{10}^V + \tilde{\chi}_{11}^V \frac{q_1^2}{M_Z^2} + \tilde{\chi}_{13}^V \frac{q_3^2}{M_Z^2} \right), \quad (\text{A.7a})$$

$$X_{3V}^{\alpha\beta} = \epsilon^{\alpha\beta\nu\sigma} q_{2\nu} q_{3\sigma} \left( \chi_{30}^V + \chi_{31}^V \frac{q_1^2}{M_Z^2} + \chi_{33}^V \frac{q_3^2}{M_Z^2} \right) + (q_3^2 - q_1^2) g^{\alpha\beta} \left( \tilde{\chi}_{30}^V + \tilde{\chi}_{31}^V \frac{q_1^2}{M_Z^2} + \tilde{\chi}_{33}^V \frac{q_3^2}{M_Z^2} \right). \quad (\text{A.7b})$$

In the above the additional form factor coefficients  $\chi_{ij}^V$  are defined as follows:

$$\begin{aligned} \chi_{10}^Z &= \frac{\eta_{\tilde{B}W}}{t_W}, & \chi_{11}^Z &= -\frac{\eta_{G+}}{2t_W} + \frac{t_W \eta_{G-}}{2}, & \chi_{30}^Z &= \frac{\eta_{\tilde{B}W}}{t_W}, & \chi_{31}^Z &= \frac{\eta_{G+}}{2t_W} - \frac{t_W \eta_{G-}}{2}, \\ \chi_{10}^\gamma &= \frac{\eta_{\tilde{B}W}}{2}, & \chi_{11}^\gamma &= -\frac{\eta_{G+}}{2} - \frac{\eta_{G-}}{2}, & \chi_{30}^\gamma &= \frac{\eta_{\tilde{B}W}}{2}, & \chi_{31}^\gamma &= \frac{\eta_{G+}}{2} - \frac{t_W^2 \eta_{G-}}{2}, \\ \tilde{\chi}_{10}^Z &= -\frac{\eta_{BW}}{2t_{2W}} + \frac{\eta_{WW}}{4} - \eta_{BB}, & \tilde{\chi}_{11}^Z &= \frac{\eta_{\tilde{G}+}}{4s_{2W}}, & \chi_{13}^Z &= -\frac{\eta_{\tilde{G}+}}{4s_{2W}}, \\ \tilde{\chi}_{30}^Z &= \frac{\eta_{BW}}{2t_{2W}} - \frac{\eta_{WW}}{4} + \eta_{BB}, & \tilde{\chi}_{31}^Z &= \frac{\eta_{\tilde{G}+}}{4s_{2W}}, & \chi_{33}^Z &= -\frac{\eta_{\tilde{G}+}}{4s_{2W}}, \\ \tilde{\chi}_{10}^\gamma &= -\frac{\eta_{BW}}{4} + \frac{t_W \eta_{WW}}{8} + \frac{\eta_{BB}}{2t_W}, & \tilde{\chi}_{11}^\gamma &= \frac{\eta_{\tilde{G}-}}{8c_W^2}, & \tilde{\chi}_{13}^\gamma &= -\frac{\eta_{\tilde{G}+}}{8c_W^2} - \frac{\eta_{\tilde{G}-}}{8c_W^2}, \\ \tilde{\chi}_{30}^\gamma &= \frac{\eta_{BW}}{4} - \frac{t_W \eta_{WW}}{8} - \frac{\eta_{BB}}{2t_W}, & \tilde{\chi}_{31}^\gamma &= \frac{\eta_{\tilde{G}-}}{8c_W^2}, & \tilde{\chi}_{33}^\gamma &= -\frac{\eta_{\tilde{G}+}}{8c_W^2} - \frac{\eta_{\tilde{G}-}}{8c_W^2}, \end{aligned} \quad (\text{A.8})$$

where  $\eta_j = v^2 M_Z^2 / [\Lambda_j^4]$ ,  $t_W = s_W / c_W$ ,  $t_{2W} = s_{2W} / c_{2W}$ , and  $(s_{2W}, c_{2W}) = (\sin 2\theta_W, \cos 2\theta_W)$ . Using the on-shell conditions for the initial/final-state fermions, we can readily prove that the contributions of  $X_{1V}^{\beta\mu}$  and  $X_{3V}^{\alpha\beta}$  to the physical processes of the present study vanish, so they are not needed for this work, but we list them here for completeness.

Finally, we clarify the difference between our new nTGC form factor formulation and the conventional nTGC form factor formulation [7]. Since there is no conventional form factor formulation for the doubly off-shell nTGVs  $Z^* \gamma V^*$  (with only  $\gamma$  on-shell) given in the literature [7][8], we compare our new formulation and the conventional formulation [7] for the nTGVs  $Z \gamma V^*$  when both  $Z$  and  $\gamma$  are on-shell. The conventional form factor parametrization of the CPC and CPV neutral triple gauge vertices  $\tilde{\Gamma}_{Z\gamma V^*}^{\alpha\beta\mu}$  yield the following formulae [7]:

$$\tilde{\Gamma}_{Z\gamma V^*}^{\alpha\beta\mu(\text{CPC})} = \frac{e(q_3^2 - M_V^2)}{M_Z^2} \left[ h_3^V q_{2\nu} \epsilon^{\alpha\beta\mu\nu} + \frac{h_4^V}{M_Z^2} q_2^\alpha q_{3\nu} q_{2\sigma} \epsilon^{\beta\mu\nu\sigma} \right], \quad (\text{A.9a})$$

$$\tilde{\Gamma}_{Z\gamma V^*}^{\alpha\beta\mu(\text{CPV})} = \frac{e(q_3^2 - M_V^2)}{M_Z^2} \left[ h_1^V (q_2^\alpha g^{\mu\beta} - q_2^\mu g^{\alpha\beta}) + \frac{h_2^V}{2M_Z^2} q_2^\alpha g^{\mu\beta} (M_Z^2 - q_3^2) \right]. \quad (\text{A.9b})$$

We found in [1] that the conventional CPC form factor  $h_4^V$  of Eq.(A.9a) is incompatible with the spontaneous breaking of the full electroweak gauge group  $\text{SU}(2)_W \otimes \text{U}(1)_Y \rightarrow \text{U}(1)_{\text{em}}$ , and leads to unphysically large high-energy behaviors. Hence we must introduce a new form factor  $h_5^V$  as in Eq.(A.10a) for matching consistently with the broken phase results originating from the CPC dimension-8 operators (2.2a)-(2.2b) and (2.3a)-(2.3b) of the SMEFT that respect the underlying electroweak  $\text{SU}(2)_W \otimes \text{U}(1)_Y$  gauge symmetry. Furthermore, we find that the conventional CPV form factor  $h_2^V$  of Eq.(A.9b) is incompatible with the spontaneous breaking of the full electroweak gauge group  $\text{SU}(2)_W \otimes \text{U}(1)_Y \rightarrow \text{U}(1)_{\text{em}}$  and also causes unphysically large high-energy behavior. Seeking a consistent formulation, we introduce another new form factor  $h_6^V$  as in Eq.(A.10b) to match with the broken phase results originating from the CPV dimension-8 operators (2.2c)-(2.2e) and (2.3c)-(2.3d) of the

SMEFT that respect the full underlying electroweak gauge symmetry. We then present the extended nTGC form factor formulations for both the CPC case [1] and the CPV case:

$$\Gamma_{Z\gamma V^*}^{\alpha\beta\mu(\text{CPC})} = \frac{e(q_3^2 - M_V^2)}{M_Z^2} \left[ \left( h_3^V + h_5^V \frac{q_3^2}{M_Z^2} \right) q_{2\nu} \epsilon^{\alpha\beta\mu\nu} + \frac{h_4^V}{M_Z^2} q_2^\alpha q_{3\nu} q_{2\sigma} \epsilon^{\beta\mu\nu\sigma} \right], \quad (\text{A.10a})$$

$$\begin{aligned} \Gamma_{Z\gamma V^*}^{\alpha\beta\mu(\text{CPV})} &= \frac{e(q_3^2 - M_V^2)}{M_Z^2} \left[ \left( h_1^V + h_6^V \frac{q_3^2}{M_Z^2} \right) (q_2^\alpha g^{\mu\beta} - q_2^\mu g^{\alpha\beta}) + \frac{h_2^V}{2M_Z^2} q_2^\alpha g^{\mu\beta} (M_Z^2 - q_3^2) \right] \\ &= \frac{e(q_3^2 - M_V^2)}{M_Z^2} \left[ h_1^V (q_2^\alpha g^{\mu\beta} - q_2^\mu g^{\alpha\beta}) + \frac{h_2^V M_Z^2 q_2^\alpha g^{\mu\beta} - 2h_6^V q_3^2 q_2^\mu g^{\alpha\beta}}{2M_Z^2} + \frac{2h_6^V - h_2^V}{2M_Z^2} q_3^2 q_2^\alpha g^{\mu\beta} \right], \end{aligned} \quad (\text{A.10b})$$

where the form factor coefficients  $h_{1,2,3,4}^V$  are the conventional form factors [7] and the form factor terms  $\propto h_5^V$  and  $h_6^V$  belong to our extension. We observe that the form factor coefficients  $(h_4^V, h_5^V)$  (CPC) and  $(h_2^V, h_6^V)$  (CPV) are subject to further constraints due to the matching with the broken phase results of the corresponding dimension-8 nTGC operators that respect the full  $\text{SU}(2)_W \otimes \text{U}(1)_Y$  electroweak gauge symmetry. These constraints ensure that for each scattering amplitude the nTGC form factor contributions have the same high-energy behaviors as those of the corresponding dimension-8 nTGC operators. For this, we make a precise matching between the above nTGC form factor formulae (A.10a)-(A.10b) and the dimension-8 nTGC operators (2.2)-(2.3). From these we derive the following nontrivial relations between the nTGC form factor coefficients:

$$h_4^V = 2h_5^V, \quad h_2^V = 2h_6^V, \quad (\text{A.11a})$$

$$h_4^Z = \frac{c_W}{s_W} h_4^\gamma, \quad h_2^Z = \frac{c_W}{s_W} h_2^\gamma. \quad (\text{A.11b})$$

Imposing these relations, we can further express the formulae (A.10a) and (A.10b) as follows:

$$\Gamma_{Z\gamma V^*}^{\alpha\beta\mu(\text{CPC})} = \frac{e(q_3^2 - M_V^2)}{M_Z^2} \left[ \left( h_3^V + h_4^V \frac{q_3^2}{2M_Z^2} \right) q_{2\nu} \epsilon^{\alpha\beta\mu\nu} + \frac{h_4^V}{M_Z^2} q_2^\alpha q_{3\nu} q_{2\sigma} \epsilon^{\beta\mu\nu\sigma} \right], \quad (\text{A.12a})$$

$$\Gamma_{Z\gamma V^*}^{\alpha\beta\mu(\text{CPV})} = \frac{e(q_3^2 - M_V^2)}{M_Z^2} \left[ h_1^V (q_2^\alpha g^{\mu\beta} - q_2^\mu g^{\alpha\beta}) + h_2^V \frac{M_Z^2 q_2^\alpha g^{\mu\beta} - q_3^2 q_2^\mu g^{\alpha\beta}}{2M_Z^2} \right]. \quad (\text{A.12b})$$

Applying naive power counting for the individual contributions of the nTGC form factors of Eqs (A.10a)-(A.10b) to the scattering amplitude for  $f\bar{f} \rightarrow Z\gamma$ , we deduce the size of each individual contribution as follows:

$$\mathcal{T}[Z_T\gamma_T](\text{CPC}) = h_3^V O(E^3) + h_5^V O(E^4), \quad (\text{A.13a})$$

$$\mathcal{T}[Z_L\gamma_T](\text{CPC}) = h_3^V O(E^3) + h_4^V O(E^5) + h_5^V O(E^5), \quad (\text{A.13b})$$

$$\mathcal{T}[Z_T\gamma_T](\text{CPV}) = h_1^V O(E^3) + h_6^V O(E^4), \quad (\text{A.13c})$$

$$\mathcal{T}[Z_L\gamma_T](\text{CPV}) = h_1^V O(E^3) + h_2^V O(E^5) + h_6^V O(E^5). \quad (\text{A.13d})$$

We note that the form factors  $h_4^V$  and  $h_2^V$  do not contribute to the amplitudes with final state  $Z_T\gamma_T$ . This is because the  $h_4^V$  and  $h_2^V$  vertices in Eqs.(A.10a)-(A.10b) contain the momentum  $q_2^\alpha = -(q_1^\alpha + q_3^\alpha)$ , and thus the contraction  $q_1^\alpha \epsilon_{T\alpha}^Z(q_1)$  vanishes due to the on-shell condition of  $Z$ , and the other contraction  $q_3^\alpha \epsilon_{T\alpha}^Z(q_1)$  vanishes due to the fact that the  $s$ -channel momentum  $q_3^\alpha$  has no spatial component and the transverse polarization vector  $\epsilon_{T\alpha}^Z$  has no time component.

Inspecting the scattering amplitudes of Eq.(A.13), we note that for the final state  $Z_L\gamma_T$ , the largest individual contributions of  $O(E^5)$  arise from the form factors  $(h_4^V, h_5^V)$  for the CPC case, as shown in Eq.(A.13b), and from the form factors  $(h_2^V, h_6^V)$  for the CPV case as shown in Eq.(A.13d). We have verified explicitly that upon imposing the matching constraints  $h_4^V = 2h_5^V$  (CPC case) and  $h_2^V = 2h_6^V$



(CPV case) of Eq.(A.11a), the sum of the individual leading contributions exhibits an exact energy cancellation  $O(E^5) \rightarrow O(E^3)$  for each amplitude. Thus, the nonzero leading contributions behave as  $O(E^4)$  and arise from the final state  $Z_T \gamma_T$  instead. The large energy cancellations  $O(E^5) \rightarrow O(E^3)$  can be understood by applying the equivalence theorem (ET) [14] to the high-energy scattering process  $f \bar{f} \rightarrow Z_L \gamma_T$ . For  $E \gg M_Z$ , the ET gives:

$$\mathcal{T}[Z_L, \gamma_T] = \mathcal{T}[-i\pi^0, \gamma_T] + B, \quad (\text{A.14})$$

where the longitudinal gauge boson  $Z_L$  absorbs the would-be Goldstone boson  $\pi^0$  through the Higgs mechanism, and the residual term  $B = \mathcal{T}[v^\mu Z_\mu, \gamma_T]$  is suppressed by the quantity  $v^\mu \equiv \epsilon_L^\mu - q_Z^\mu/M_Z = O(M_Z/E_Z)$  [14]. We note that the ET (A.14) cannot be directly applied to the conventional form factor formulation (A.9), because it obeys only the gauge symmetry  $U(1)_{\text{em}}$  and does not respect the full electroweak gauge symmetry of the SM. More generally, the form factor formulation is normally given in the broken phase of the electroweak gauge symmetry and contains no would-be Goldstone boson. We should apply the ET to the electroweak gauge-invariant formulation of the nTGCs which can be derived only from the dimension-8 operators as in Eqs.(2.2)-(2.3). Thus, we can analyze the allowed leading energy-dependences of the amplitudes (A.13b) and (A.13d) by applying the ET to the contributions of the dimension-8 nTGC operators in Eqs.(2.2)-(2.3). From these, we find that only the Higgs-related nTGC operators in Eq.(2.2) could contribute to the Goldstone amplitude  $\mathcal{T}[-i\pi^0, \gamma_T]$  with a leading energy-dependence  $O(E^3)$  that corresponds to the form factor  $h_3^Z$  or  $h_1^Z$ . The operators  $\mathcal{O}_{G_\pm}$  or  $\tilde{\mathcal{O}}_{G_\pm}$  do not contribute to the Goldstone boson amplitude  $\mathcal{T}[-i\pi^0, \gamma_T]$ , but they contribute the largest residual term  $B = O(E^3)$ . With these results, we apply the ET (A.14) and deduce that in Eqs.(A.13b) and (A.13d) the individual leading terms of  $O(E^5)$  due to the form factors ( $h_4^V, h_5^V$ ) (CPC case) or ( $h_2^V, h_6^V$ ) (CPV case) must exactly cancel with each other, from which we derive the the following conditions:

$$h_4^V/h_5^V = 2, \quad h_2^V/h_6^V = 2, \quad (\text{A.15})$$

in agreement with Eq.(A.11a). From the above, we further conclude that the final nonzero leading amplitude is  $O(E^4)$  as in  $\mathcal{T}[Z_T \gamma_T]$  and is contributed by  $h_5^V$  in the CPC case in Eq.(A.13a) or by  $h_6^V$  in the CPV case in Eq.(A.13c).

Next we consider the scattering process  $f \bar{f} \rightarrow Z^* \gamma \rightarrow f' \bar{f}' \gamma$  with an off-shell  $Z^*$ , as studied in the main text. Using our doubly off-shell nTGV formulase (2.5) and (2.7), we can count the leading energy-dependence for the contribution of each form factor as follows:

$$\mathcal{T}[f' \bar{f}' \gamma_T](\text{CPC}) = h_{31}^\gamma O(E^1) + \hat{h}_3^\gamma O(E^3) + \hat{h}_3^Z O(E^1) + \hat{h}_4 O(E^3), \quad (\text{A.16a})$$

$$\mathcal{T}[f' \bar{f}' \gamma_T](\text{CPV}) = h_{11}^\gamma O(E^1) + \hat{h}_1^\gamma O(E^3) + \hat{h}_1^Z O(E^1) + \hat{h}_2 O(E^3). \quad (\text{A.16b})$$

We see that the nonzero leading energy dependence is  $O(E^3)$ , contributed by the form factors ( $\hat{h}_3^\gamma, \hat{h}_4$ ) and ( $\hat{h}_1^\gamma, \hat{h}_2$ ). This is in contrast with the on-shell amplitudes  $\mathcal{T}[Z_T \gamma_T]$  in Eqs.(A.13a) and (A.13c), which have nonzero leading energy-dependences  $O(E^4)$ , contributed by  $h_5^V$  and  $h_6^V$ .

As shown in Eq.(2.5) of Section 2, we find that the contribution of  $\hat{h}_{3,1}^\gamma$  to the nTGVs is enhanced by a large factor  $q_1^2/M_Z^2$  from the off-shell decays  $Z^*(q_1) \rightarrow \nu \bar{\nu} \gamma$ , whereas the contributions of  $\hat{h}_{3,1}^Z$  and  $\hat{h}_{4,2}$  are dominated by on-shell  $Z$  decays, so including off-shell  $Z^*$  decays does not cause important changes in their sensitivity reaches. Hence, for studying the form factors  $\hat{h}_{4,2}$ , we can consider the  $Z \gamma V^*$  nTGVs, and make a quantitative comparison between our new form factor formulation (A.12) and the conventional form factor formulae (A.9) [7] via the production channel  $pp(q\bar{q}) \rightarrow Z \gamma \rightarrow \nu \bar{\nu} \gamma$  at hadron colliders. We present this comparison in Table 3, where the third row (red color) depicts the sensitivity reaches for  $\hat{h}_{4,2}$  obtained by using our nTGV formula (A.12), and the last two rows (blue color) show the sensitivity reaches for  $h_{4,2}$  that would be obtained by using the (incorrect) conventional nTGV formulas (A.9) [7]. Table 3 demonstrates that the sensitivity reaches for the conventional nTGC

$\sqrt{s}$	13 TeV				100 TeV		
$\mathcal{L}(\text{ab}^{-1})$	0.14	0.3	3		3	10	30
$ \hat{h}_{4,2}  \times 10^6$	11	8.5	4.2	$ \hat{h}_{4,2}  \times 10^9$	4.5	2.9	2.0
$ h_{4,2}^Z  \times 10^6$	0.47	0.37	0.19	$ h_{4,2}^Z  \times 10^{11}$	2.6	1.7	1.2
$ h_{4,2}^\gamma  \times 10^6$	0.54	0.43	0.22	$ h_{4,2}^\gamma  \times 10^{11}$	2.9	1.9	1.4

Table 3: Comparisons of the  $2\sigma$  sensitivity reaches for the form factors ( $\hat{h}_4, \hat{h}_2$ ) formulated in the SMEFT (in red color) and for the conventional form factors ( $h_4^V, h_2^V$ ) respecting only  $U(1)_{\text{em}}$  (in blue color), derived from the reaction  $pp(q\bar{q}) \rightarrow Z\gamma \rightarrow \nu\bar{\nu}\gamma$  at the LHC (13 TeV) and a 100 TeV  $pp$  collider, with the indicated integrated luminosities. As discussed in the text, the form-factor limits in blue color are included for illustration only, as they are incompatible with the spontaneous breaking of the SM electroweak gauge symmetry, and hence are invalid.

form factors  $h_{4,2}^V$  are erroneously stronger than those for our new formulation (A.12) by about a factor of  $O(20)$  at the LHC and by about a factor of  $O(170)$  at the 100 TeV  $pp$  collider. In Ref. [1], we also clarified this issue for the case of analyzing the CPC form factors of the nTGVs  $Z\gamma V^*$  via the on-shell  $Z\gamma$  production process  $pp(q\bar{q}) \rightarrow Z\gamma \rightarrow \ell^+\ell^-\gamma$ .

## B Cross Sections for CPC and CPV nTGC Contributions

In this Appendix, we present the cross section formulae for the reaction  $q\bar{q} \rightarrow Z^*\gamma$  in terms of the SM contribution ( $\sigma_0$ ), the interference between the SM and the nTGC contributions ( $\sigma_1$ ), and the squared part of the nTGC contributions ( $\sigma_2$ ), which are used in Eq.(3.2) of the main text:

$$\sigma(q\bar{q} \rightarrow Z^*\gamma) = \sigma_0 + \sigma_1 + \sigma_2. \quad (\text{B.1})$$

The individual cross section terms given by

$$\sigma_0 = \frac{e^4(q_L^2 + q_R^2)Q^2[-(\hat{s} - M_{Z^*}^2)^2 - 2(\hat{s}^2 + M_{Z^*}^4) \ln \sin \frac{\delta}{2}]}{8\pi s_W^2 c_W^2 (\hat{s} - M_{Z^*}^2) \hat{s}^2}, \quad (\text{B.2a})$$

$$\begin{aligned} \sigma_1 = & -\frac{e^4 Q q_L T_3 (\hat{s} - M_{Z^*}^2)}{16\pi s_W^2 c_W^2 M_{Z^*}^2 \hat{s}} \bar{h}_4 - \frac{e^4 Q (q_L x_L^Z - q_R x_R^Z) (\hat{s}^2 - M_{Z^*}^4)}{16\pi s_W^2 c_W^2 M_{Z^*}^2 \hat{s}^2} \bar{h}_3^Z \\ & + \frac{e^4 Q (q_L x_L^A - q_R x_R^A) (\hat{s}^2 - M_{Z^*}^4)}{16\pi s_W^3 c_W M_{Z^*}^2 \hat{s}^2} \bar{h}_3^\gamma, \end{aligned} \quad (\text{B.2b})$$

and

$$\sigma_2 = \sigma_2^{44} + \sigma_{2Z}^{33} + \sigma_{2A}^{33} + \sigma_{2Z}^{43} + \sigma_{2A}^{43} + \sigma_{2ZA}^{33}, \quad (\text{B.3a})$$

$$\sigma_2^{44} = \frac{e^4 T_3^2 (\hat{s} + M_{Z^*}^2) (\hat{s} - M_{Z^*}^2)^3}{768\pi s_W^2 c_W^2 M_{Z^*}^8 \hat{s}} [(\bar{h}_2)^2 + (\bar{h}_4)^2], \quad (\text{B.3b})$$

$$\sigma_{2Z}^{33} = \frac{e^4 [Q^2 s_W^4 + (T_3 - Q s_W^2)^2] (\hat{s} + M_{Z^*}^2) (\hat{s} - M_{Z^*}^2)^3}{192\pi s_W^2 c_W^2 M_{Z^*}^6 \hat{s}^2} [(\bar{h}_1^Z)^2 + (\bar{h}_3^Z)^2], \quad (\text{B.3c})$$

$$\sigma_{2A}^{33} = \frac{e^4 Q^2 (\hat{s} + M_{Z^*}^2) (\hat{s} - M_{Z^*}^2)^3}{96\pi M_{Z^*}^6 \hat{s}^2} [(\bar{h}_1^\gamma)^2 + (\bar{h}_3^\gamma)^2], \quad (\text{B.3d})$$

$\sqrt{s}$	13 TeV				100 TeV		
$\mathcal{L}(\text{ab}^{-1})$	0.14	0.3	3		3	10	30
$ \hat{h}_{4,2}  \times 10^6$	9.6	7.5	3.8	$ \hat{h}_{4,2}  \times 10^9$	3.9	2.6	1.8
$ \hat{h}_{3,1}^Z  \times 10^4$	1.9	1.5	0.80	$ \hat{h}_{3,1}^Z  \times 10^7$	6.1	4.2	3.0
$ \hat{h}_{3,1}^\gamma  \times 10^4$	1.6	1.2	0.65	$ \hat{h}_{3,1}^\gamma  \times 10^7$	0.94	0.62	0.44
$ h_{31,11}^\gamma  \times 10^4$	2.2	1.8	0.94	$ h_{31,11}^\gamma  \times 10^7$	7.1	4.9	3.5

Table 4: Combined sensitivity reaches on probing the CPC and CPV nTGC form factors at the  $2\sigma$  level, as obtained by analyzing the reactions  $pp(q\bar{q}) \rightarrow Z^*\gamma \rightarrow \nu\bar{\nu}\gamma$  and  $pp(q\bar{q}) \rightarrow Z\gamma \rightarrow \ell^+\ell^-\gamma$  at the LHC (13 TeV) and the 100 TeV  $pp$  collider, for the indicated integrated luminosities. In the last two rows, the  $\hat{h}_{3,1}^\gamma$  sensitivities (red color) are significantly higher than those of  $h_{31,11}^\gamma$  (blue color) because the former contains the off-shell contributions from  $\nu\bar{\nu}\gamma$  channel as enhanced by  $Z^*$ -momentum-square ( $q_1^2$ ) and the latter does not.

$$\sigma_{2Z}^{43} = \frac{e^4 T_3 (T_3 - Qs_W^2) (\hat{s} - M_{Z^*}^2)^3}{96\pi s_W^2 c_W^2 M_{Z^*}^6 \hat{s}} (\bar{h}_2 \bar{h}_1^Z + \bar{h}_4 \bar{h}_3^Z), \quad (\text{B.3e})$$

$$\sigma_{2A}^{43} = \frac{e^4 Q T_3 (\hat{s} - M_{Z^*}^2)^3}{96\pi s_W c_W M_{Z^*}^6 \hat{s}} (\bar{h}_2 \bar{h}_1^\gamma + \bar{h}_4 \bar{h}_3^\gamma), \quad (\text{B.3f})$$

$$\sigma_{2ZA}^{33} = \frac{e^4 Q (T_3 - 2Qs_W^2) (\hat{s} + M_{Z^*}^2) (\hat{s} - M_{Z^*}^2)^3}{96\pi s_W c_W M_{Z^*}^6 \hat{s}^2} (\bar{h}_1^Z \bar{h}_1^\gamma + \bar{h}_3^Z \bar{h}_3^\gamma), \quad (\text{B.3g})$$

where

$$\bar{h}_{1,3}^Z = \hat{h}_{1,3}^Z \frac{M_{Z^*}^2}{M_Z^2}, \quad \bar{h}_{1,3}^\gamma = h_{1,3} \frac{M_{Z^*}^2}{M_Z^2} + \hat{h}_{1,3} \frac{M_{Z^*}^4}{M_Z^4}, \quad \bar{h}_{2,4} = \hat{h}_{2,4} \frac{M_{Z^*}^4}{M_Z^4}. \quad (\text{B.4})$$

In the above, the squared-mass  $M_{Z^*}^2 = q_1^2$  with  $q_1$  being the  $Z^*$  momentum, and the coefficients  $(q_L, q_R) = (T_3 - Qs_W^2, -Qs_W^2)$ ,  $(x_L^Z, x_R^Z) = (T_3 - Qs_W^2, -Qs_W^2)$ , and  $(x_L^A, x_R^A) = -Qs_W^2(1, 1)$  denote the (left, right)-handed gauge couplings between quarks and the  $Z$  boson.

Finally, we combine the sensitivity reaches on probing the CPC and CPV nTGC form factors by using the bounds derived from the reaction  $pp(q\bar{q}) \rightarrow Z^*\gamma \rightarrow \nu\bar{\nu}\gamma$  (given in Table 1 of the main text) and the reaction  $pp(q\bar{q}) \rightarrow Z\gamma \rightarrow \ell^+\ell^-\gamma$ . We analyzed the  $\nu\bar{\nu}\gamma$  channel in [1] only for CPC nTGCs, and for the current combined analysis we further include the CPV nTGCs. We present the combined sensitivity reaches on probing the CPC and CPV nTGC form factors at the  $2\sigma$  level, for both the on-going LHC and the projected 100 TeV  $pp$  collider, as shown in Table 4. We find that the sensitivity reaches on the form factors  $\hat{h}_{4,2}$ ,  $\hat{h}_{3,1}^Z$ , and  $h_{31,11}^\gamma$  are comparable for both  $\nu\bar{\nu}\gamma$  and  $\ell^+\ell^-\gamma$  channels, where the  $\nu\bar{\nu}\gamma$  channel has higher sensitivities than the  $\ell^+\ell^-\gamma$  channel by about (20–30)% at the LHC and the 100 TeV  $pp$  collider, and thus their combined sensitivities have visible improvements. On the other hand, the sensitivity reaches on the form factors  $\hat{h}_{3,1}^\gamma$  via the  $\nu\bar{\nu}\gamma$  channel are significantly higher than those via the  $\ell^+\ell^-\gamma$  channel by about 93% at the LHC and by a large factor of  $O(10)$  at the 100 TeV  $pp$  collider, because of the major off-shell enhancement on the  $\nu\bar{\nu}\gamma$  signals as we demonstrated in the main text. This explains why the combined sensitivity reaches on  $\hat{h}_{3,1}^\gamma$  (shown in Table 4 and marked in red color) are dominated by the  $\nu\bar{\nu}\gamma$  channel and remain nearly the same as the sensitivities of the  $\nu\bar{\nu}\gamma$  channel alone (shown in Table 1 of the main text). We also analyzed the combined sensitivity reaches on the new physics cutoff scale  $\Lambda_j$  for each given nTGC operator  $\mathcal{O}_j$ . Since the nTGC contribution to the signal cross section is dominated by the  $\sigma_2$

$\sqrt{s}$	13 TeV			100 TeV		
$\mathcal{L} \text{ (ab}^{-1}\text{)}$	0.14	0.3	3	3	10	30
$\Lambda_{G+} \text{ (CPC)}$	3.4	3.6	4.2	23	26	29
$\Lambda_{G-} \text{ (CPC)}$	1.2	1.3	1.5	7.7	8.5	9.3
$\Lambda_{\tilde{B}W} \text{ (CPC)}$	1.3	1.4	1.6	5.6	6.1	6.6
$\Lambda_{\widetilde{B}W} \text{ (CPC)}$	1.5	1.6	1.9	6.4	7.0	7.6
$\Lambda_{\tilde{G}+} \text{ (CPV)}$	2.8	3.0	3.5	20	22	24
$\Lambda_{\tilde{G}-} \text{ (CPV)}$	1.0	1.1	1.3	6.5	7.2	7.8
$\Lambda_{WW} \text{ (CPV)}$	0.96	1.0	1.2	4.0	4.4	4.8
$\Lambda_{WB} \text{ (CPV)}$	1.1	1.2	1.4	4.8	5.2	5.7
$\Lambda_{BB} \text{ (CPV)}$	1.4	1.5	1.7	5.8	6.4	7.0

Table 5: Combined sensitivity reaches on the new physics scales  $\Lambda_j$  (in TeV) of the dimension-8 nTGC operators at  $2\sigma$  level, as obtained by analyzing the reactions  $pp(q\bar{q}) \rightarrow Z^*\gamma \rightarrow \nu\bar{\nu}\gamma$  and  $pp(q\bar{q}) \rightarrow Z\gamma \rightarrow \ell^+\ell^-\gamma$  at the LHC (13 TeV) and at a 100 TeV  $pp$  collider, with integrated luminosities  $\mathcal{L}$  as indicated.

term which is proportional to  $1/\Lambda_j^8$  (as compared to  $\sigma_2 \propto \hat{h}_j^2$  for the form factor contributions), we would expect a rather minor enhancement by  $2^{1/16} - 1 \simeq 4.4\%$  even if the two channels of  $\nu\bar{\nu}\gamma$  and  $\ell^+\ell^-\gamma$  would contribute equal statistical significance. We present in Table 5 the combined sensitivity reaches on the new physics scales  $\Lambda_j$  (in TeV) of the dimension-8 nTGC operators at  $2\sigma$  level. As expected, it shows that the combination of both  $\nu\bar{\nu}\gamma$  and  $\ell^+\ell^-\gamma$  channels leads to fairly minor improvements on the sensitivity reaches. Especially, there are essentially no visible improvements beyond the sensitivity bounds of the  $\nu\bar{\nu}\gamma$  channel (shown in Table 2 of the main text) for new physics scales ( $\Lambda_{G-}$ ,  $\Lambda_{\tilde{G}-}$ ), which correspond to the nTGC form factors ( $\hat{h}_3^\gamma$ ,  $\hat{h}_1^\gamma$ ). This is because the  $\nu\bar{\nu}\gamma$  channel has large off-shell enhancements for the contributions of ( $\hat{h}_3^\gamma$ ,  $\hat{h}_1^\gamma$ ) and thus the corresponding new physics scale ( $\Lambda_{G-}$ ,  $\Lambda_{\tilde{G}-}$ ), which lead to significantly higher sensitivity reaches than those of the  $\ell^+\ell^-\gamma$  channel.

## C Unitarity Constraints on CPC and CPV nTGCs

In this section, we analyze the perturbative unitarity bounds on both the CPC and CPV nTGCs through the on-shell scattering process  $f\bar{f} \rightarrow Z\gamma$  with  $f\bar{f} = q\bar{q}, e^-e^+$ . This also extends our previous unitarity analysis for the CPC nTGCs alone [1]. For the scattering amplitude of the reaction  $f\bar{f} \rightarrow Z\gamma$ , We make the partial-wave expansion of the nTGC contributions:

$$a_J = \frac{1}{32\pi} e^{i(\nu' - \nu)\phi} \int_{-1}^1 d(\cos\theta) d_{\nu'\nu}^J(\cos\theta) \mathcal{T}_{\text{nTGC}}^{s_f s_{\bar{f}}, \lambda_Z \lambda_\gamma}, \quad (\text{C.21})$$

where the differences of initial/final state helicities are given by  $\nu = s_f - s_{\bar{f}} = \pm 1$  and  $\nu' = \lambda_Z - \lambda_\gamma = 0, \pm 1$ , respectively. For the current collider analysis it is sufficient to treat the initial-state fermions ( $f, \bar{f}$ ) (light quarks or leptons) as massless. So we deduce  $s_f = -s_{\bar{f}}$ , leading to  $\nu = \pm 1$ . This means that the  $J=1$  partial wave gives the leading contribution. The relevant

$E_{\text{CM}}(\text{TeV})$	0.25	0.5	1	3	5	25	40
$\Lambda_{G+}$	0.078	0.16	0.31	0.93	1.6	7.8	12
$\Lambda_{G-}$	0.050	0.084	0.14	0.32	0.47	1.6	2.2
$\Lambda_{\tilde{B}W}$	0.058	0.098	0.16	0.37	0.55	1.8	2.6
$\Lambda_{\widetilde{B}W}$	0.069	0.12	0.20	0.44	0.65	2.2	3.1
$\Lambda_{\tilde{G}+}$	0.065	0.13	0.26	0.79	1.3	6.5	10
$\Lambda_{\tilde{G}-}$	0.042	0.071	0.12	0.27	0.40	1.3	1.9
$\Lambda_{WW}$	0.041	0.069	0.12	0.26	0.39	1.3	1.8
$\Lambda_{WB}$	0.051	0.086	0.14	0.33	0.48	1.6	2.3
$\Lambda_{BB}$	0.069	0.12	0.20	0.44	0.65	2.2	3.1
$ h_{4,2} $	33	2.0	0.13	$1.6 \times 10^{-3}$	$2.0 \times 10^{-4}$	$3.3 \times 10^{-7}$	$5.0 \times 10^{-8}$
$ h_{3,1}^Z $	53	6.6	0.83	0.031	$6.6 \times 10^{-3}$	$5.3 \times 10^{-5}$	$1.3 \times 10^{-5}$
$ h_{3,1}^\gamma $	53	6.6	0.83	0.031	$6.6 \times 10^{-3}$	$5.3 \times 10^{-5}$	$1.3 \times 10^{-5}$

Table 6: *Unitarity bounds on the new physics scale  $\Lambda_j$  (in TeV) of the dimension-8 nTGC operators and on the nTGC form factors  $h_j^V$  including both the CPC and CPV cases. These bounds are derived for various sample values of the c.m. energy  $E_{\text{CM}}$  of the reaction  $q\bar{q} \rightarrow Z\gamma$  or  $e^-e^+ \rightarrow Z\gamma$  that are relevant to the present collider study.*

Wigner  $d$  functions are given by  $d_{1,0}^1 = -\frac{1}{\sqrt{2}} \sin \theta$  and  $d_{1,\pm 1}^1 = \frac{1}{2}(1 \pm \cos \theta)$ , whereas the general relation  $d_{m,m'}^J = d_{-m,-m'}^J$  holds.

With these, we impose the inelastic unitarity condition [21] on each given partial-wave amplitude  $|a_J^{\text{ine}}| < \frac{1}{2}$  for  $J=1$ , and derive the following perturbative unitarity bounds on the leading contributions of the nTGC form factors:

$$|h_{4,2}| < \frac{24\sqrt{2}\pi v^2 M_Z^2}{s_W c_W s^2}, \quad |h_{3,1}^Z| < \frac{6\sqrt{2}\pi v^2 M_Z}{s_W c_W (T_3 - Q s_W^2) s^{3/2}}, \quad |h_{3,1}^\gamma| < \frac{6\sqrt{2}\pi v^2 M_Z}{s_W^2 c_W^2 |Q| s^{3/2}}, \quad (\text{C.22})$$

where  $Q$  is the electric charge of the initial state fermions,  $T_3 = \pm \frac{1}{2}$  for left-handed fermions and  $T_3 = 0$  for right-handed fermions. Then, we impose the inelastic unitarity condition on the leading contribution of each dimension-8 nTGC operator to the partial wave amplitude of the reaction  $f\bar{f} \rightarrow Z\gamma$ , and derive the following inelastic unitarity bounds:

$$\Lambda_{G+} > \frac{\sqrt{s}}{(24\sqrt{2}\pi)^{1/4}}, \quad \Lambda_{G-} > \left( \frac{s_W^2 |Q| M_Z}{12\sqrt{2}\pi} \right)^{\frac{1}{4}} (\sqrt{s})^{\frac{3}{4}}, \quad \Lambda_{\tilde{B}W} > \left( \frac{\widehat{T}_3 |M_Z|}{12\sqrt{2}\pi} \right)^{\frac{1}{4}} (\sqrt{s})^{\frac{3}{4}}, \quad (\text{C.23a})$$

$$\Lambda_{\widetilde{B}W} > \left( \frac{2|Q| M_Z}{\omega} \right)^{\frac{1}{4}} (\sqrt{s})^{\frac{3}{4}}, \quad \Lambda_{\tilde{G}+} > \frac{\sqrt{s}}{(48\sqrt{2}\pi)^{1/4}}, \quad \Lambda_{\tilde{G}-} > \left( \frac{s_W |Q| M_Z}{2c_W \omega} \right)^{\frac{1}{4}} (\sqrt{s})^{\frac{3}{4}}, \quad (\text{C.23b})$$

$$\Lambda_{WW} > \left( \frac{|T_3| M_Z}{2\omega} \right)^{\frac{1}{4}} (\sqrt{s})^{\frac{3}{4}}, \quad \Lambda_{BW} > \left( \frac{|\widehat{Q}| M_Z}{s_W c_W \omega} \right)^{\frac{1}{4}} (\sqrt{s})^{\frac{3}{4}}, \quad \Lambda_{BB} > \left( \frac{2|Q - T_3| M_Z}{\omega} \right)^{\frac{1}{4}} (\sqrt{s})^{\frac{3}{4}}, \quad (\text{C.23c})$$

where we have defined  $\omega = 12\sqrt{2}\pi/(s_W c_W)$ ,  $\widehat{T}_3 = T_3 - Q s_W^2$ , and  $\widehat{Q} = Q s_W^2 + T_3(1 - 2s_W^2)$ . With these we derive the numerical unitarity bounds on the new physics scale  $\Lambda_j$  of each

nTGC dimension-8 operator and on each nTGC form factor  $h_j^V$ , including both the CPC and CPV cases. We summarize these unitarity bounds in Table 6 for a set of sample values of the relevant center-of-mass energy  $E_{\text{CM}}(=\sqrt{s})$  of the scattering process  $f\bar{f} \rightarrow Z\gamma$  with  $f\bar{f} = q\bar{q}, e^-e^+$ . Table 6 demonstrates that these unitarity bounds on  $\Lambda_j$  and  $h_j^V$  are much weaker than our current collider bounds (shown in Tables 1-2 and Tables 4-5) and thus do not affect our collider analyses.

## References

- [1] J. Ellis, H.-J. He, R.-Q. Xiao, Phys. Rev. D 107 (2023) 035005, no.3, [arXiv:2206.11676].
- [2] J. Ellis, H.-J. He, and R.-Q. Xiao, Science China (Phys. Mech. Astron.) 64 (2021) 221062, no.2, [arXiv:2008.04298].
- [3] J. Ellis, S.-f. Ge, H.-J. He, and R.-Q. Xiao, Chin. Phys. C 44 (2020) 063106, no.6, [arXiv:1902.06631].
- [4] V. Khachatryan *et al.*, [CMS Collaboration], Phys. Lett. B 760 (2016) 448-468 [arXiv:1602.07152 [hep-ex]].
- [5] M. Aaboud *et al.*, [ATLAS Collaboration], JHEP 12 (2018) 010 [arXiv:1810.04995 [hep-ex]].
- [6] E.g., S. Jahedi, arXiv:2305.11266 [hep-ph]; S. Spor, E. Gurkanli and M. Köksal, arXiv:2302.08245 [hep-ph]; S. Jahedi and J. Lahiri, JHEP 04 (2023) 085 [arXiv:2212.05121 [hep-ph]]; S. Spor, Nucl. Phys. B 991 (2023) 116198 [arXiv:2207.11585 [hep-ph]]; A. Senol, S. Spor, E. Gurkanli, V. Cetinkaya, H. Denizli, and M. Köksal, Eur. Phys. J. Plus 137 (2022) 1354, no.12 [arXiv:2205.02912 [hep-ph]]; Q. Fu, J. C. Yang, C. X. Yue, and Y. C. Guo, Nucl. Phys. B 972 (2021) 115543 [arXiv:2102.03623 [hep-ph]]. A. Biekötter, P. Gregg, F. Krauss, and M. Schönherr, Phys. Lett. B 817 (2021) 136311 [arXiv:2102.01115 [hep-ph]]; A. Senol, H. Denizli, A. Yilmaz, I. Turk Cakir, K. Y. Oyulmaz, O. Karadeniz, and O. Cakir, Nucl. Phys. B 935 (2018) 365 [arXiv:1805.03475 [hep-ph]]; R. Rahaman and R. K. Singh, Eur. Phys. J. C 77 (2017) 521, no.8 [arXiv:1703.06437 [hep-ph]]; Eur. Phys. J. C 76 (2016) 539, no.10 [arXiv:1604.06677 [hep-ph]].
- [7] G. J. Gounaris, J. Layssac, and F. M. Renard, Phys. Rev. D 61 (2000) 073013 [arXiv:hep-ph/9910395 [hep-ph]].
- [8] C. Degrande, JHEP 1402 (2014) 101 [arXiv:1308.6323 [hep-ph]].
- [9] For reviews, see John Ellis, arXiv:2105.14942 [hep-ph], in the conference proceedings of “Beyond Standard Model: From Theory to Experiment” (BSM-2021), Zewail City, Egypt, March 29-31, 2021; I. Brivio and M. Trott, Phys. Rept. 793 (2019) 1 [arXiv:1706.08945 [hep-ph]].
- [10] B. Grzadkowski, M. Iskrzynski, M. Misiak, and J. Rosiek, JHEP 10 (2010) 085 [arXiv:1008.4884 [hep-ph]]; and references therein.



- [11] See, e.g., J. Ellis, V. Sanz, and T. You, JHEP 1407 (2014) 036 [Xiv:1404.3667 [hep-ph]] and JHEP 1503 (2015) 157 [arXiv:1410.7703 [hep-ph]]; H.-J. He, J. Ren, and W. Yao, Phys. Rev. D 93 (2016) 015003 [arXiv:1506.03302 [hep-ph]]; J. Ellis and T. You, JHEP 03 (2016) 089 [arXiv:1510.04561 [hep-ph]]; S.-F. Ge, H.-J. He, and R.-Q. Xiao, JHEP 10 (2016) 007 [arXiv:1603.03385]; J. de Blas et al., JHEP 12 (2016) 135 [arXiv:1608.01509 [hep-ph]]; F. Ferreira, B. Fuks, V. Sanz, and D. Sengupta, Eur. Phys. J. C 77 (2017) 675 [arXiv:1612.01808 [hep-ph]]; J. Ellis, P. Roloff, V. Sanz, and T. You, JHEP 05 (2017) 096 [arXiv:1701.04804 [hep-ph]]; G. Durieux, C. Grojean, J. Gu and K. Wang, JHEP 09 (2017) 014 [arXiv:1704.02333 [hep-ph]]; T. Barklow et al., Phys. Rev. D 97 (2018) 053003 [arXiv:1708.08912 [hep-ph]]; C. W. Murphy, Phys. Rev. D 97 (2018) 015007 [arXiv:1710.02008 [hep-ph]]; J. Ellis, C. W. Murphy, V. Sanz, and T. You, JHEP 06 (2018) 146 [arXiv:1803.03252]; G. N. Remmen and N. L. Rodd, JHEP 12 (2019) 032 [arXiv:1908.09845 [hep-ph]]; A. Gutierrez-Rodriguez, M. Koksál, A. A. Billur, M. A. Hernandez-Ruiz, J. Phys. G 47 (2020) 055005 [arXiv:1910.02307 [hep-ph]]; M. Koksál, A. A. Billur, A. Gutierrez-Rodriguez, and M. A. Hernandez-Ruiz, Phys. Lett. B 808 (2020) 135661 [arXiv:1910.06747 [hep-ph]]; J. Ellis, M. Madigan, K. Mimasu, V. Sanz, and T. You, JHEP 04 (2021) 279 [arXiv:2012.02779 [hep-ph]]. and references therein.
- [12] We emphasize that the conventional electroweak form factor formulation imposes only the  $U(1)$  gauge symmetry of QED, and is in general *incompatible* with the SMEFT framework, which takes into account the full  $SU(2) \otimes U(1)$  electroweak gauge symmetry of the SM. We stress that it is important to match precisely the form factors with the corresponding SMEFT operators in the broken phase, which can place additional nontrivial constraints on the structure of the form factors as a result of the spontaneous electroweak symmetry breaking of the SM. We demonstrate this for our correct formulation of the nTGC form factors in Section 3.
- [13] We note that the CMS [4] and ATLAS [5] collaborations also measured the CPC nTGC form factor  $h_4^V$  using the conventional formula, which gives rise to unphysically large high-energy behavior [1].
- [14] For a comprehensive review, see H. J. He, Y.P. Kuang and C.P. Yuan, arXiv:hep-ph/9704276 and DESY-97-056, in the Proceedings of the Workshop on “Physics at the TeV Energy Scale”, vol.72 (1996), p.119. See also, H. J. He and W.B. Kilgore, Phys. Rev. D 55 (1997) 1515; H. J. He, Y. P. Kuang and C. P. Yuan, Phys. Rev. D 51 (1995) 6463; Phys. Rev. D 55 (1997) 3038; H. J. He, Y. P. Kuang and X. Li, Phys. Lett. B 329 (1994) 278; Phys. Rev. D 49 (1994) 4842; Phys. Rev. Lett. 69 (1992) 2619; and references therein.
- [15] H. L. Lai *et al.* [CTEQ Collaboration], Eur. Phys. J. C 12 (2000) 375-392 [hep-ph/9903282 [hep-ph]]; T. J. Hou *et al.* [CTEQ Collaboration], Phys. Rev. D 103 (2021) 014013, no.1 [1912.10053 [hep-ph]].
- [16] We find that the situation is different for probing the nTGCs at high-energy  $e^+e^-$  colliders [2][3][17], where the interference contribution can dominate over the squared contribution.
- [17] J. Ellis, H.-J. He, and R.-Q. Xiao, in preparation.
- [18] B. Ananthanarayan, J. Lahiri, M. Patra and S. D. Rindani, JHEP 08 (2014) 124 [arXiv:1404.4845 [hep-ph]].

- [19] We thank Shu Li for discussing the ATLAS analyses and advising us how to estimate the ATLAS detection efficiency.
- [20] G. Cowan, K. Cranmer, E. Gross, and O. Vitells, *Eur. Phys. J. C* **71** (2011) 1554 [arXiv:1007.1727 [physics.data-an]].
- [21] D. A. Dicus and H.-J. He, *Phys. Rev. D* **71** (2005) 093009 [arXiv:hep-ph/0409131]; and *Phys. Rev. Lett.* **94** (2005) 221802 [arXiv:hep-ph/0502178].